Поляризационные эффекты в столкновениях тяжелых ионов

В. Рябов, ЛРЯФ ОФВЭ

Relativistic heavy-ion collisions

- Interacting system evolves through different stages:
  early pre-equilibrium phase → formation of hot and dense partonic matter
  → phase transition to the excited hadronic gas as the system expands and cools down
  → chemical freeze-out → kinetic freeze-out → detectors

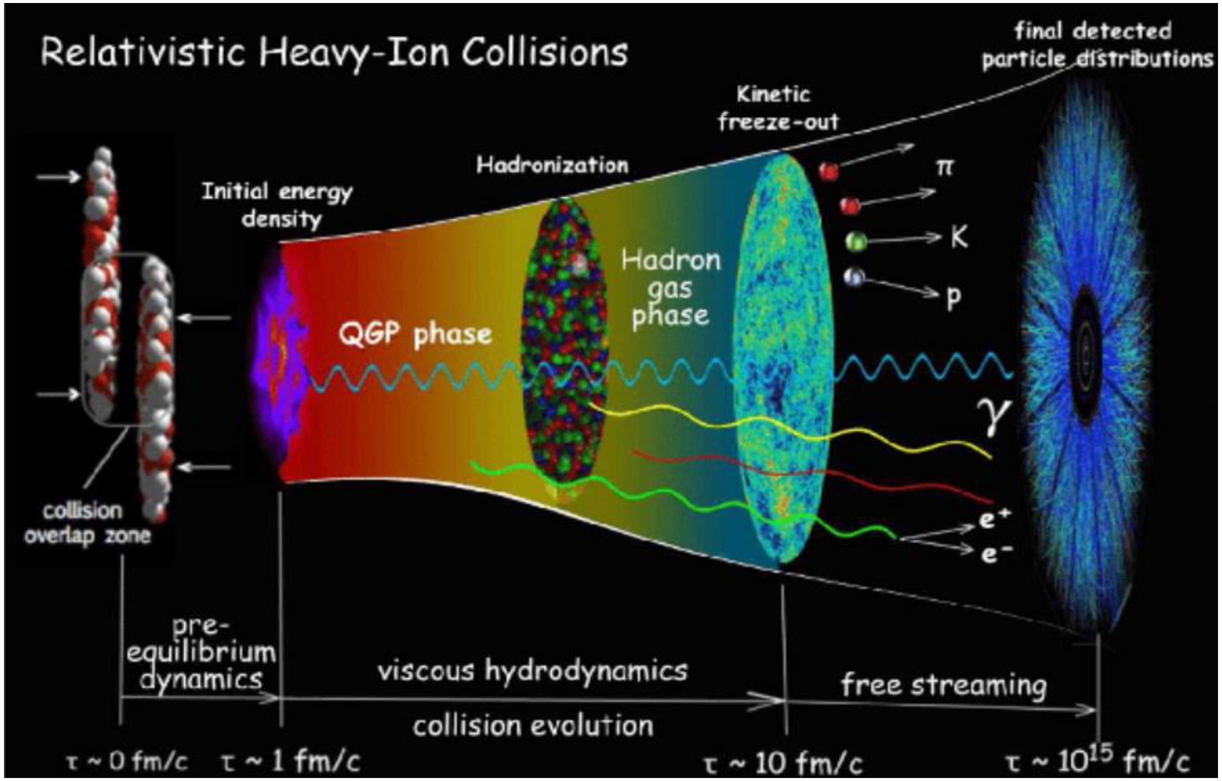

Properties of the medium - I

- Properties of the sQGP in heavy-ion collisions:
  - ✓ extends ~ over a size of colliding nuclei
  - ✓ highest temperatures and energy densities

$$R_{AA}(p_T) = \frac{d^2N^{AA}/dp_T d\eta}{\langle N_{binary}\rangle d^2N^{pp}/dp_T d\eta}$$

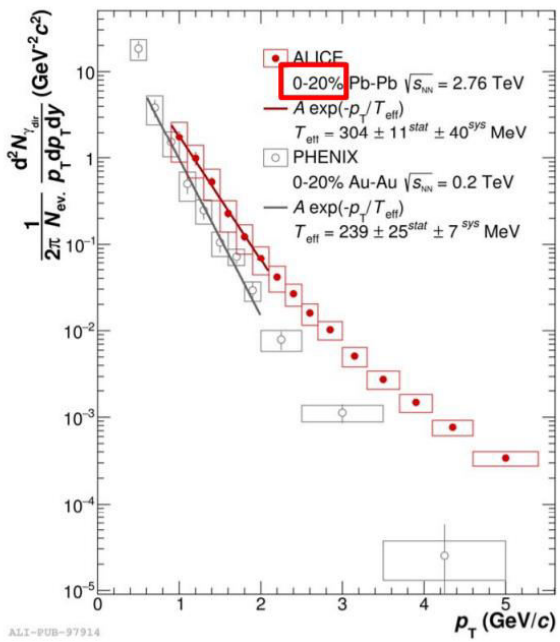

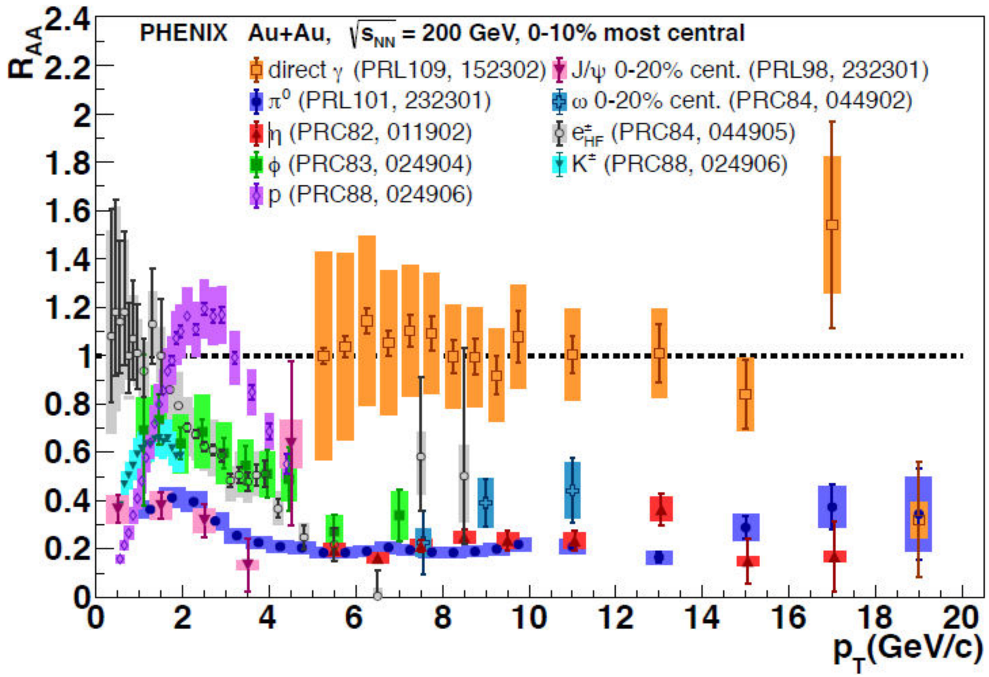

- T_{eff} ~ 240 MeV in AuAu@200 GeV
- T_{eff} ~ 300 MeV in PbPb@2760 GeV
  - → the hottest medium ever
  - → $T_{eff} >> T_c$

- R_{AA} ~ 0.2 up to 20 ГэВ/c in central A_A
- Absence of suppression for γ_{dir} and hadrons in p-A
- Same suppression for light hadrons → partonic level
- Heavy c-quarks are also suppressed
- Theory: ε > 15 ГэВ/фм^3; dN_g/dy > 1100

Properties of the medium - II

- Properties of the sQGP in heavy-ion collisions:
  - ✓ extends ~ over a size of colliding nuclei
  - ✓ highest temperatures and energy densities
  - ✓ fast thermalization, nearly perfect fluid, η/s close to quantum bound ($\hbar/4\pi$)
  - ✓ partonic degrees of freedom

$$\frac{dN_{\rm ch}}{d\phi} \propto 1 + 2v_1 \cos(\phi - \Psi_1) + 2v_2 \cos[2(\phi - \Psi_2)] + \cdots$$

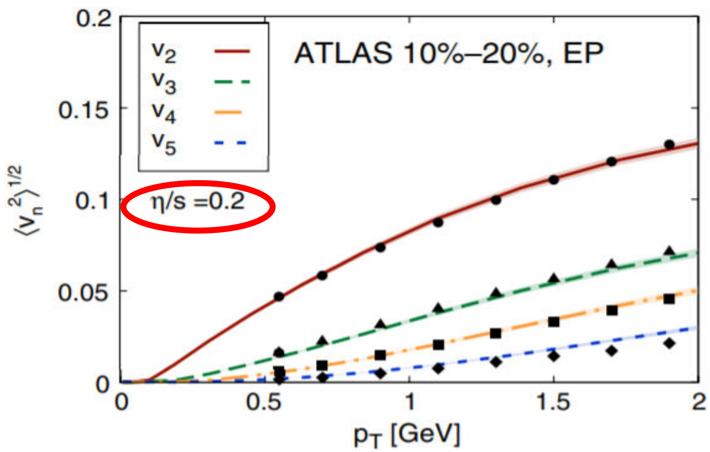

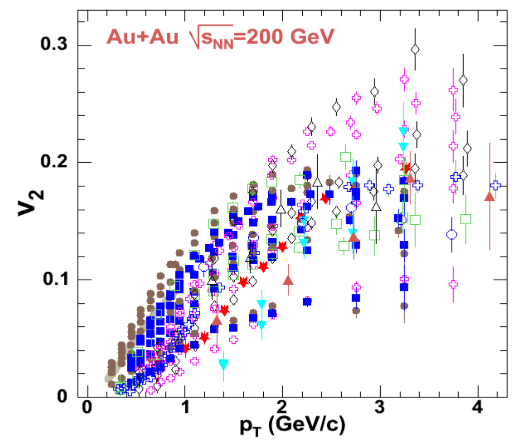

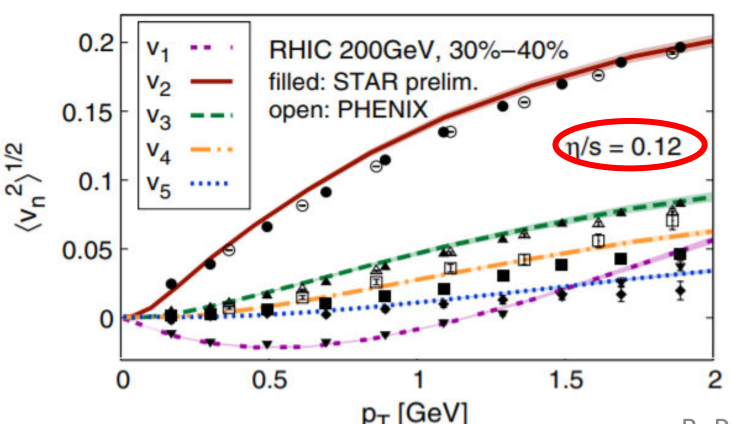

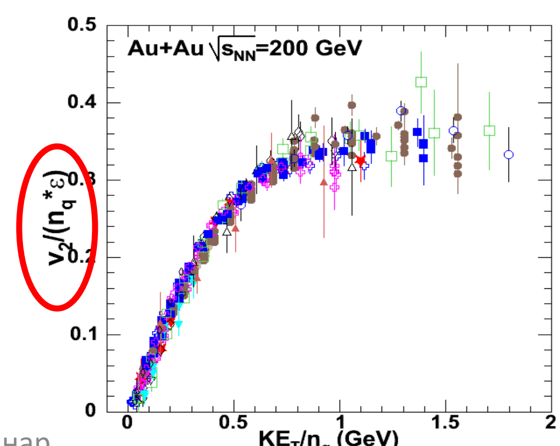

Non-central collisions

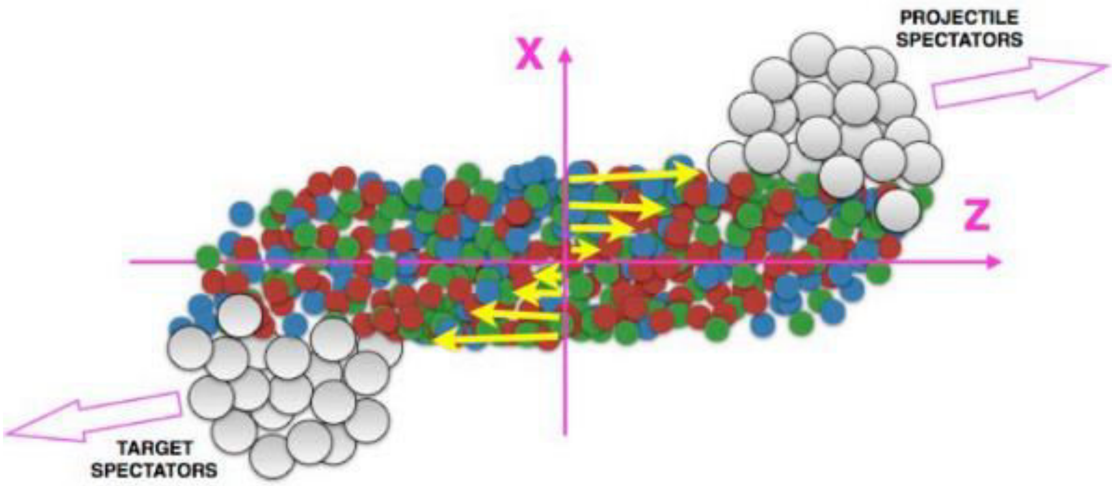

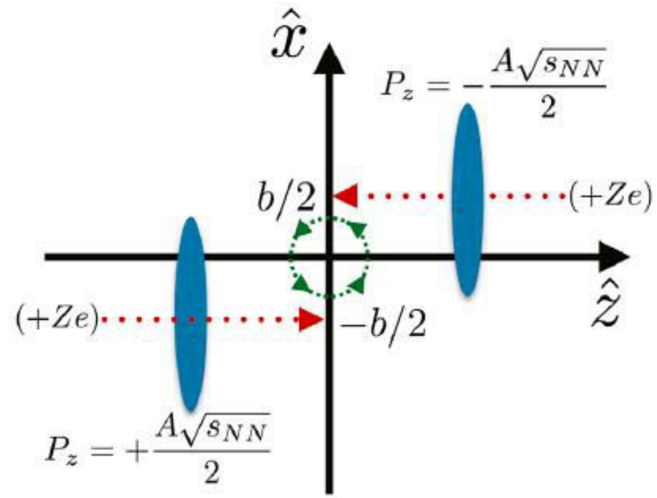

- Huge angular momentum for the system in non-central collisions at high energy:

$$L_y = |\bar{r} \times \bar{p}| \sim \frac{Ab\sqrt{s_{NN}}}{2} \sim 10^4\text{-}10^5\ \hbar$$

- Angular momentum of the system can polarize the system constituents (quarks)

  → global polarization → polarization of particles in the final state

Global polarization

Phys.Rev.Lett.94:102301,2005; Erratum-ibid.Lett.96:039901,2006

Globally Polarized Quark-gluon Plasma in Non-central $A + A$ Collisions

Zuo-Tang Liang[1] and Xin-Nian Wang[2,1]
[1]*Department of Physics, Shandong University, Jinan, Shandong 250100, China*
[2]*Nuclear Science Division, MS 70R0319, Lawrence Berkeley National Laboratory, Berkeley, California 94720*
(Dated: October 18, 2004)

Produced partons have large local relative orbital angular momentum along the direction opposite to the reaction plane in the early stage of non-central heavy-ion collisions. Parton scattering is shown to polarize quarks along the same direction due to spin-orbital coupling. Such global quark polarization will lead to many observable consequences, such as left-right asymmetry of hadron spectra, global transverse polarization of thermal photons, dileptons and hadrons. Hadrons from the decay of polarized resonances will have azimuthal asymmetry similar to the elliptic flow. Global hyperon polarization is studied within different hadronization scenarios and can be easily tested.

Barnet effect (1915)

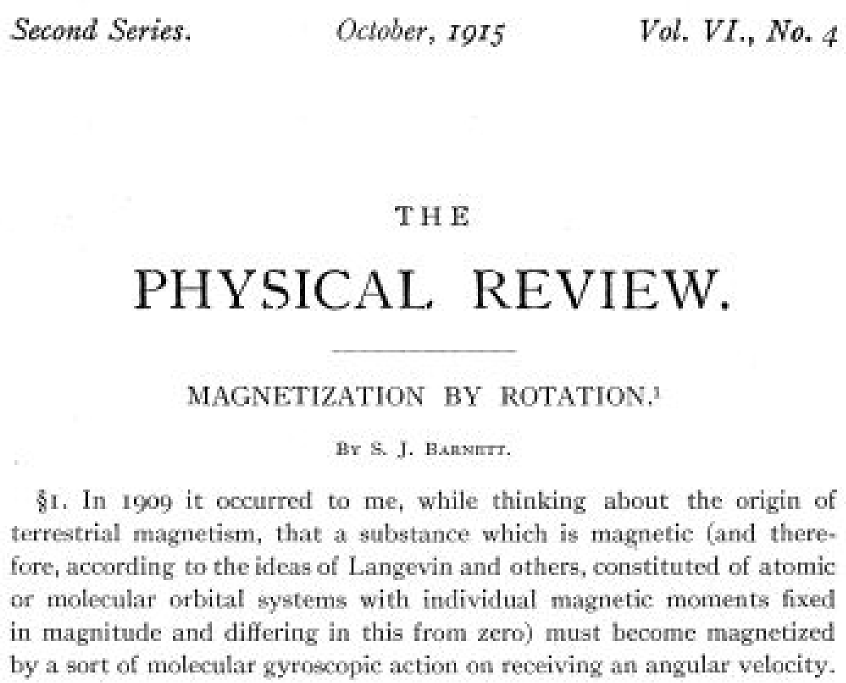

Second Series. *October, 1915* *Vol. VI., No. 4*

THE

PHYSICAL REVIEW.

MAGNETIZATION BY ROTATION.[1]

BY S. J. BARNETT.

§1. In 1909 it occurred to me, while thinking about the origin of terrestrial magnetism, that a substance which is magnetic (and therefore, according to the ideas of Langevin and others, constituted of atomic or molecular orbital systems with individual magnetic moments fixed in magnitude and differing in this from zero) must become magnetized by a sort of molecular gyroscopic action on receiving an angular velocity.

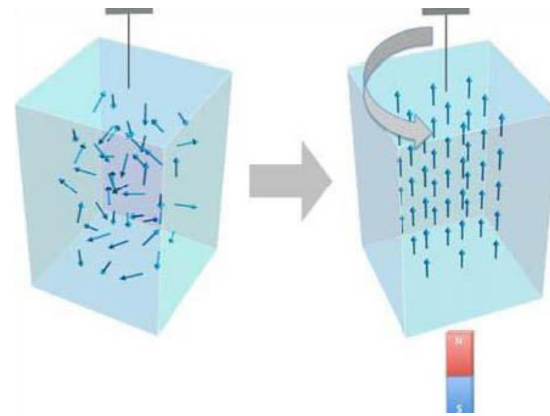

- Magnetization by rotation: macroscopic rotation (global angular momentum) → microscopic spin alignment
- M ~ ω

Spin hydrodynamic generation

Nature Physics 12, pages52–56 (2016)

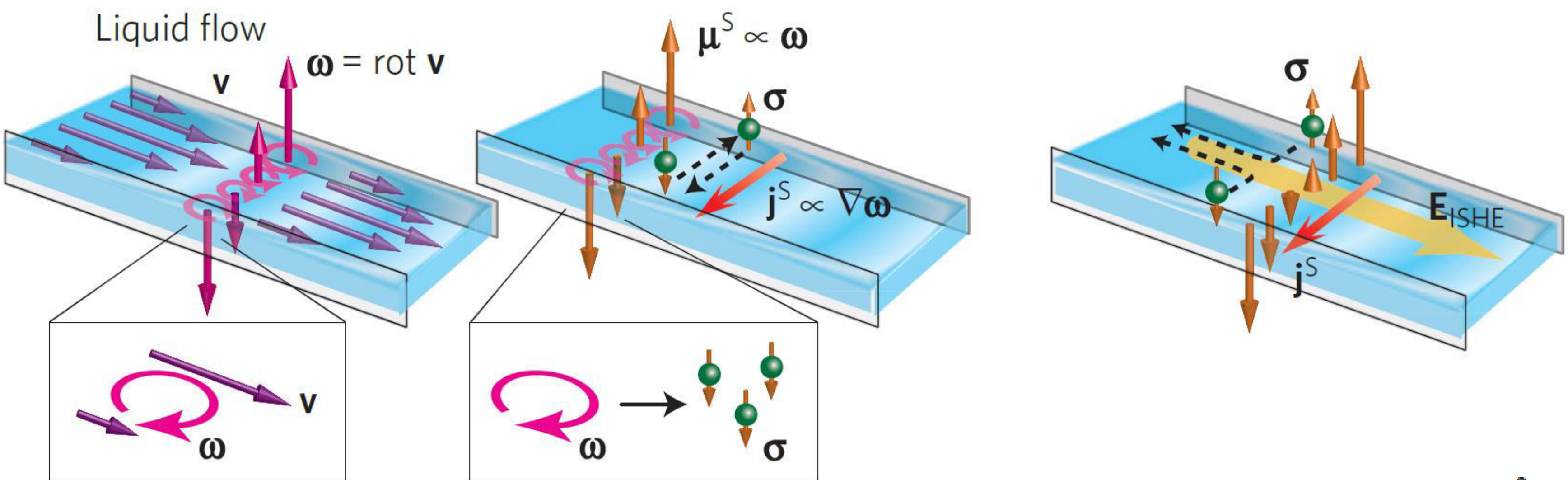

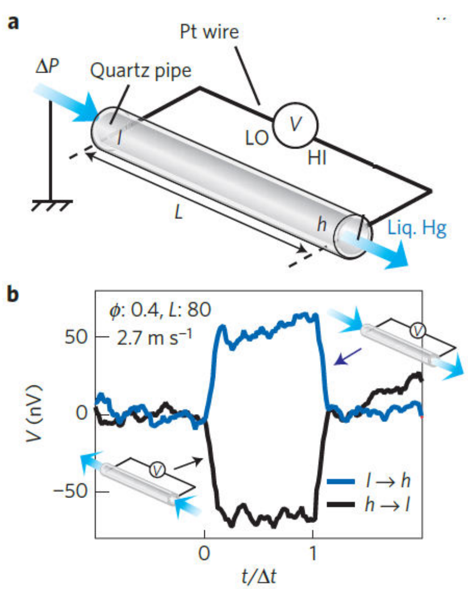

- Equation for spin voltage: $$\nabla^2 \boldsymbol{\mu}^S = \frac{1}{\lambda^2}\boldsymbol{\mu}^S - \frac{4e^2}{\sigma_0 \hbar}\xi\boldsymbol{\omega}$$

$\mu^S \equiv \mu_\uparrow - \mu_\downarrow$, where

$\mu_\uparrow$ and $\mu_\downarrow$ respectively denote the electrochemical potential for spin-up and spin-down electrons

a gradient of spin voltage drives a spin current

λ is the spin-diffusion length ξ is fluid viscosity

- Vorticity acts as a spin current source
- Viscous fluid flow → vorticity → spin polarization

Non-central collisions

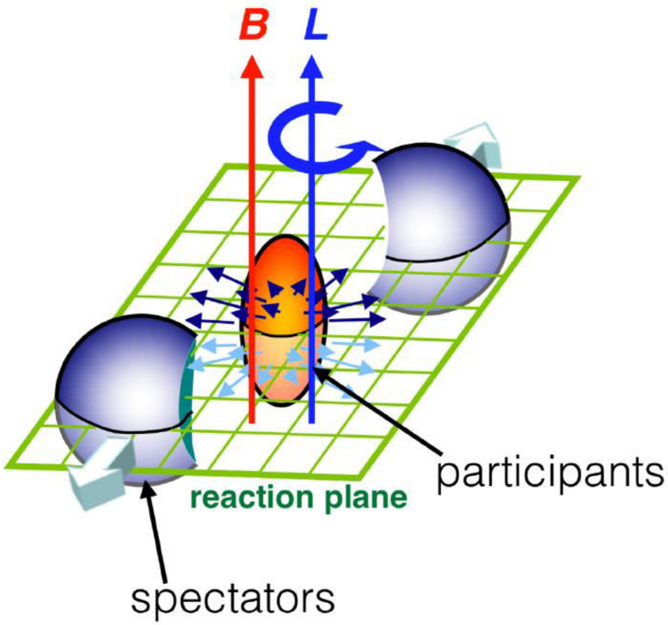

Large angular momentum due to medium rotations (PRC 77 (2008) 024906, Beccattini et al.)

Strong magnetic field (~ 10^{13} T) formed for a short period of time (NPA 803 (2008), Kharzeev et al.)

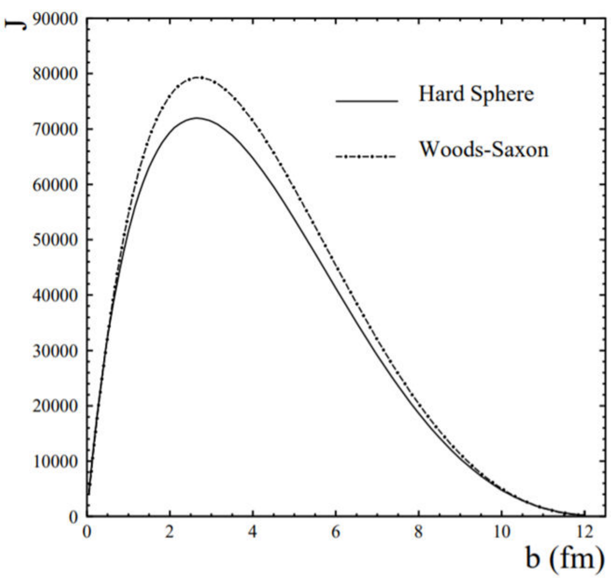

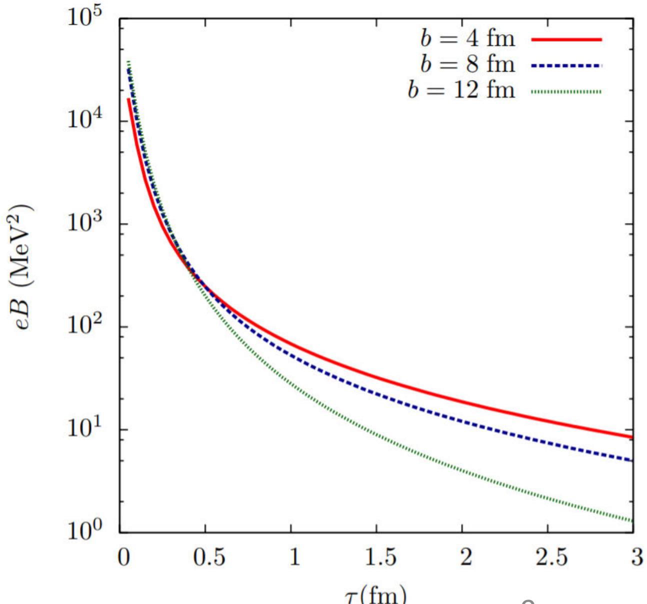

Polarization in a relativistic fluid

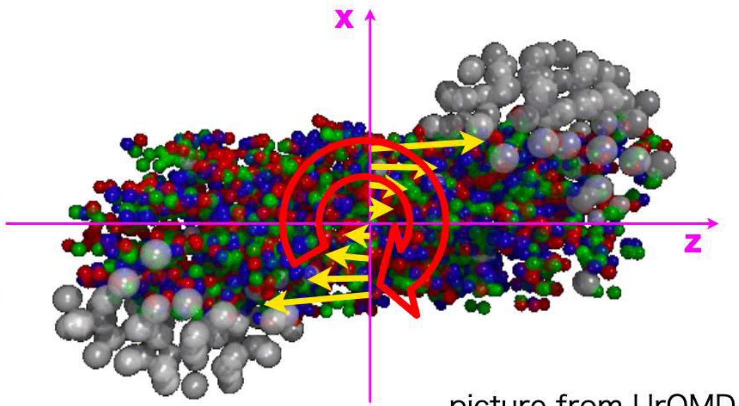

picture from UrQMD

- In a relativistic fluid at local thermodynamic equilibrium, spin polarization is driven by:

F. Becattini et al.; arXiv:2103.14621 [nucl-th]; B. Fu et al.; arXiv:2103.10403 [hep-ph]

Thermal vorticity: $\varpi_{\mu\nu} = \frac{1}{2}(\partial_\nu \beta_\mu - \partial_\mu \beta_\nu) \xrightarrow{\text{In non-relativistic limit}} \varpi \sim \omega/T$

$\beta^\mu = \frac{1}{T}u^\mu,$

β – four-temperature vector
u – four velocity, T – proper temperature

- Hydrodynamic, transport, or any other models don't have the physics ingredients to generate particle spin polarization
- Models generate hydrodynamic gradients (flow gradients, temperature gradients) → sources of vorticity
- To estimate particle polarization from vorticity → need a theoretical framework

Polarization in a relativistic fluid

- No theoretical knowledge about:
  - ✓ evolution of quark spin polarization in QGP
  - ✓ formation of a polarized hyperon from the polarized quarks
  - ✓ effect of hadronic scatterings on spin d.o.f
  - ✓ estimation of the relaxation times

- Solution: Local equilibrium formula relates the mean spin vector $S^{\mu}(p)$ of a spin ½ fermion to the vorticity sources at the hadronizationg hypersurface Σ (extension of Cooper-Frye formalism).

$$S^{\mu}(p) = -\frac{1}{8m}\epsilon^{\mu\rho\sigma\tau}p_{\tau}\frac{\int_{\Sigma} \mathrm{d}\Sigma \cdot p\, n_F(1-n_F)\varpi_{\rho\sigma}}{\int_{\Sigma} \mathrm{d}\Sigma \cdot p\, n_F}$$

$$n_F = \frac{1}{\exp[\beta \cdot p - q\mu/T] + 1}$$ - Fermi-Dirac phase-space distribution function

- Vorticity results in equal polarization for particles and antiparticles

- There are no relativistic calculations for particles with s > 1/2

Hyperon polarization

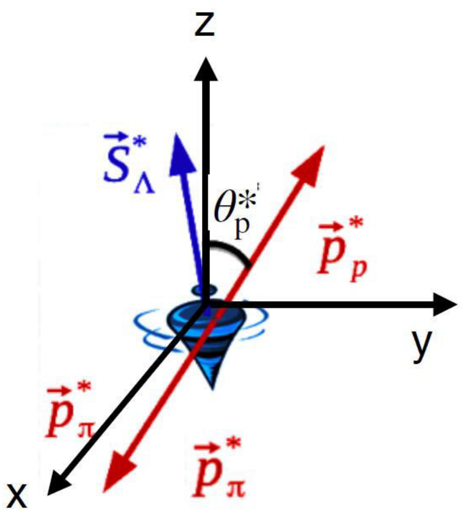

- $\Lambda \rightarrow p + \pi^-$ (BR ~ 64%, cτ ~ 8 cm), parity violating weak decay
- Daughter baryon is preferentially emitted in the direction of hyperon spin (opposite for antiparticle):

$$\frac{dN}{d\cos\theta^*} = \frac{1}{2}\left(1 + \alpha_H |\vec{\mathcal{P}}_H| \cos\theta^*\right)$$

(* denotes hyperon rest frame)

$\mathbf{P}_H$ = hyperon polarization vector

α_H = hyperon decay parameter

$\hat{\mathbf{p}}^*_p$ = unit vector along daughter baryon momentum

BESIII, Nature Phys. 15 (2019):

$\alpha_\Lambda = 0.750 \pm 0.009$

$\alpha_{\bar{\Lambda}} = -0.758 \pm 0.01$

- Polarization estimation procedure:
  - ✓ identify the reference axis
  - ✓ take a projection of the daughter proton's momentum direction on the reference axis
  - ✓ average that projection over all hyperons in all events

Global hyperon polarization (STAR)

STAR, Nature 548, 62 (2017)

S. Voloshin, T. Niida; Phys. Rev. C 94, 021901(R) (2016)

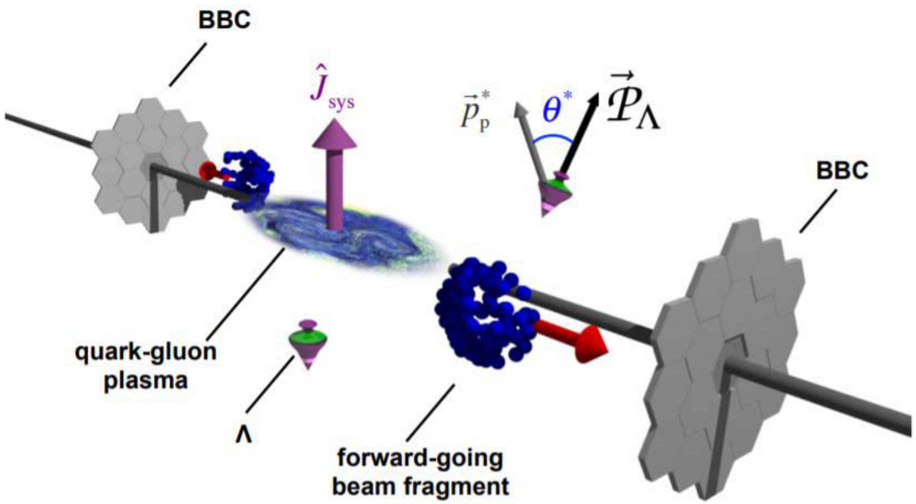

$$\overline{\mathcal{P}}_{\rm H} \equiv \langle \vec{\mathcal{P}}_{\rm H} \cdot \hat{J}_{\rm sys} \rangle = \frac{8}{\pi \alpha_{\rm H}} \frac{\left\langle \cos\left(\phi_p^* - \Psi_1\right)\right\rangle}{{\rm Res}(\Psi_1)}$$

ϕ_p^* - azimuthal angle of daughter proton in $\Lambda(\overline{\Lambda})$ rest frame

ψ_1 – observed angular momentum angle

Res(ψ_1) - resolution of ψ_1 measurements

Reconstruction of $\Lambda(\bar{\Lambda})$

- $\Lambda(\bar{\Lambda}) \rightarrow p(\bar{p})+\pi$ using identified tracks and V0 topology cuts

V0 topology:

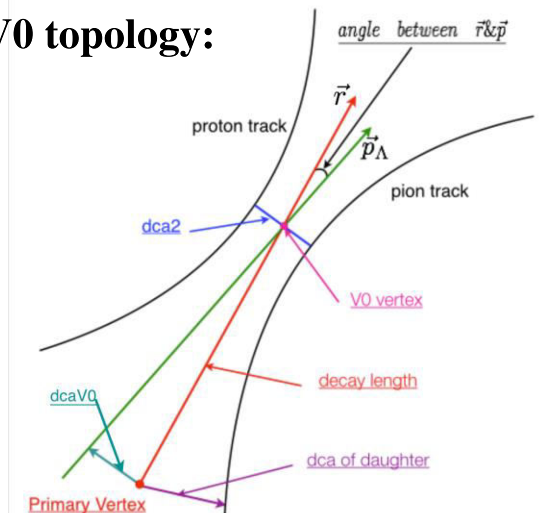

- Variables or selections:
  - ✓ opposite charge $p(\bar{p})$ and π tracks pairs identified by dE/dx, ToF
  - ✓ χ^2 of Kalman fit of track pair (how good the pair complies with hypothesis to originate from the same secondary vertex)
  - ✓ distance between tracks, < 0.5-1 cm
  - ✓ production radius (how far from the primary vertex), > 5 mm
  - ✓ α = angle between $\bar{r}$ & $\bar{p}$, $\alpha < 0.07$
  - ✓ DCA of daughter tracks (track-to-PV distance), > mm
  - ✓ decay asymmetry
  - ✓ veto on competing $K_s^0 \rightarrow \pi^+\pi^-$ decay

→ Quite a lot of variables, but most of them are correlated !!!

- Selection cuts depend on the detector capabilities and physical signals/background
- Optimized for high purity of signal and yet high efficiency of reconstruction

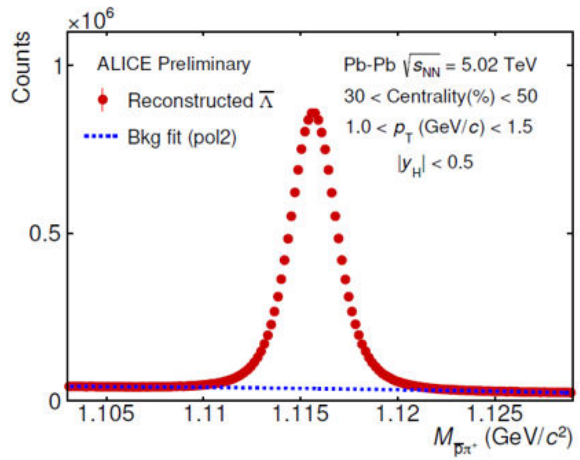

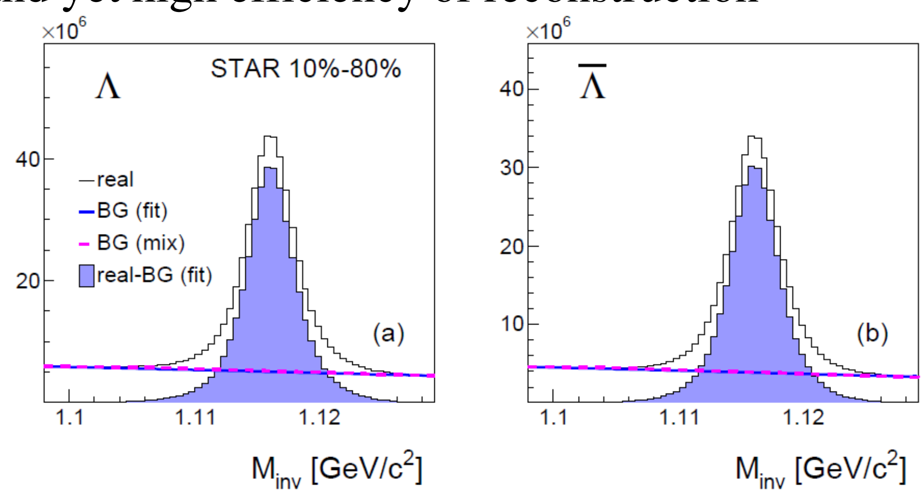

Event plane measurements

- Event plane is estimated from the azimuthal distribution of tracks (TPC) or energy in forward detectors (V0, ZDC):

$$Q_x^m = \frac{\sum E_i \cos(m\varphi_i)}{\sum E_i}, Q_y^m = \frac{\sum E_i \sin(m\varphi_i)}{\sum E_i}$$

$$\Psi_m^{EP} = \frac{1}{m} ATan2\left(Q_y^m, Q_x^m\right)$$

- For m=1 weights had different signs for backward and forward rapidity
- Event plane is a proxy for reaction plane smeared by event plane resolution

$$Res_n^2\{\Psi_n^{EP,L}, \Psi_n^{EP,R}\} = \langle \cos[n(\Psi_n^{EP,L} - \Psi_n^{EP,R})] \rangle$$

- ψ_1^{EP} is used for hyperon global polarization measurements
- ψ_2^{EP} is used for local polarization measurements

Global polarization measurement

$$\overline{\mathcal{P}}_{\mathrm{H}} \equiv \langle \vec{\mathcal{P}}_{\mathrm{H}} \cdot \hat{J}_{\mathrm{sys}} \rangle = \frac{8}{\pi \alpha_{\mathrm{H}}} \frac{\left\langle \cos\left(\phi_p^* - \Psi_1\right)\right\rangle}{\mathrm{Res}(\Psi_1)}$$

- Event plane method:
  1) number of Λ ($\bar{\Lambda}$) counted in each bin of the hyperon emission azimuthal angle relative to EP
  2) yield of Λ ($\bar{\Lambda}$) as a function of $\Psi_1 - \phi^*$ is fitted with a sine function to obtain $\langle \sin(\Psi_1 - \phi_p^*) \rangle$
- Invariant mass method:

polarization signal

$$\langle \sin(\Psi_1 - \phi_p^*) \rangle^{\mathrm{obs}} = (1 - f^{\mathrm{Bg}}(M_{\mathrm{inv}})) \langle \sin(\Psi_1 - \phi_p^*) \rangle^{\mathrm{Sg}} + f^{\mathrm{Bg}}(M_{\mathrm{inv}}) \langle \sin(\Psi_1 - \phi_p^*) \rangle^{\mathrm{Bg}}$$

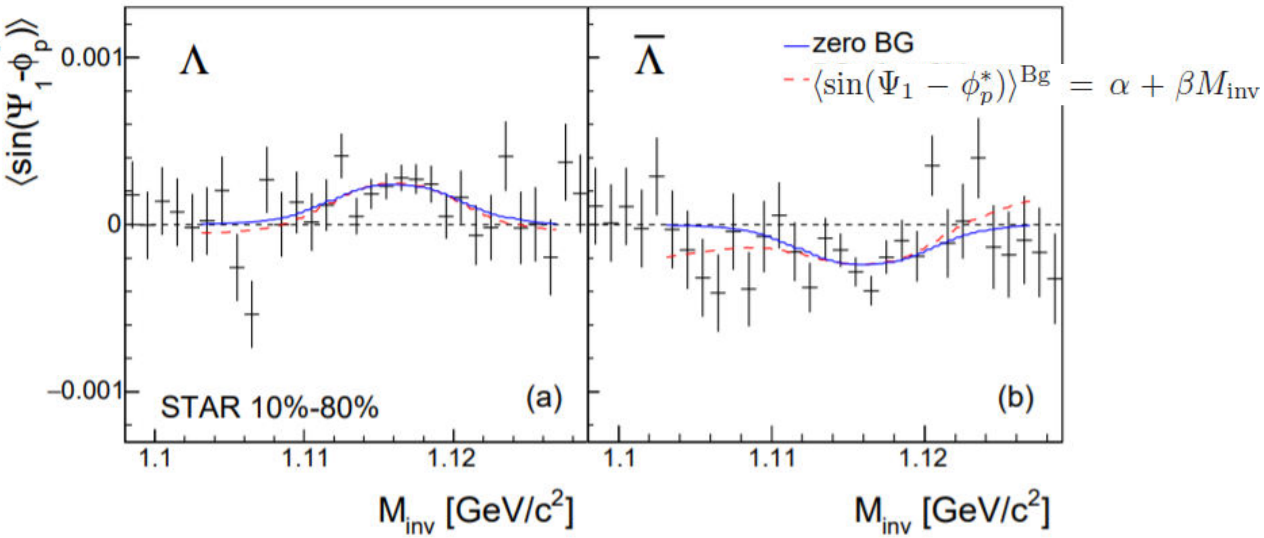

- Results from the invariant mass and event plane methods are consistent (systematics unc.)

Global polarization

EPJ Web Conf., 171 (2018) 07002; Nature 548, 62 (2017)

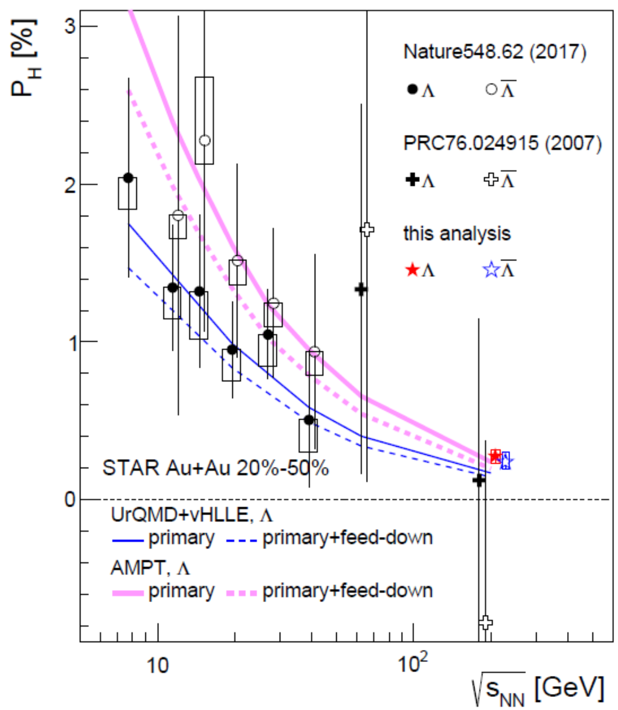

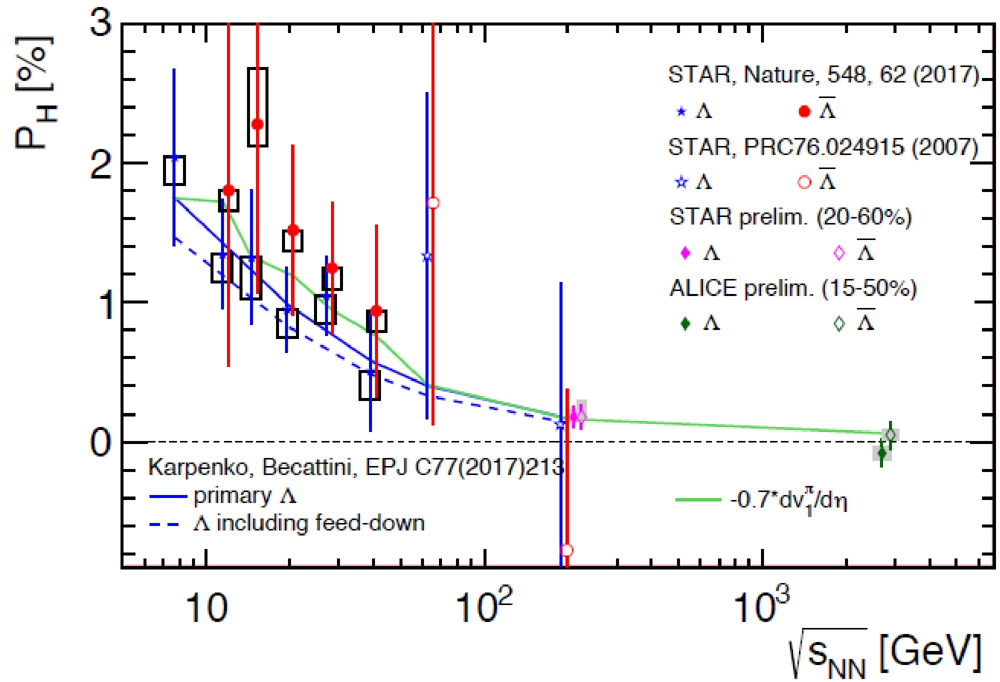

- Global polarization of hyperons experimentally observed!!!; decreases with $\sqrt{s_{NN}}$
- Feed down from Σ(1385) → Λπ, Σ^0 →Λγ; Ξ→Λπ reduces polarization by ~ 10-20%
- B estimates to explain a Λ-$\bar{\Lambda}$ difference within the range of theoretical predictions

$$P_\Lambda \simeq \frac{1}{2}\frac{\omega}{T} + \frac{\mu_\Lambda B}{T}$$

$$P_{\bar{\Lambda}} \simeq \frac{1}{2}\frac{\omega}{T} - \frac{\mu_\Lambda B}{T}$$

μ_Λ - magnetic moment

B = $(P_\Lambda - P_{\bar{\Lambda}})\cdot T/(2\,\mu_\Lambda)$ ~ $2\cdot 10^{11}$ T or eB ~ $10^{-2}\, m_\pi^2$

$(P_\Lambda - P_{\bar{\Lambda}})$ = 0.5%, T = 160 MeV at hadronization

Full energy dependence

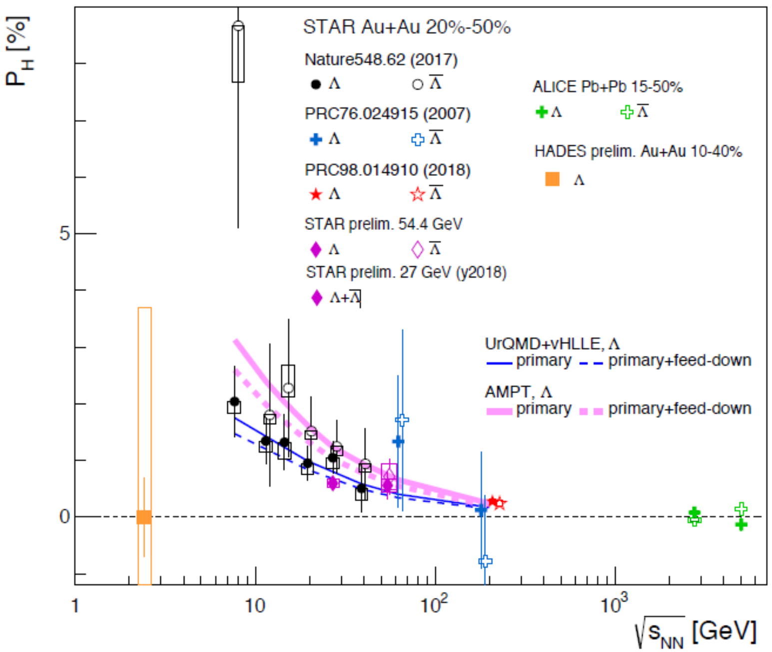

arXiv:2108.00044v2 [nucl-ex]

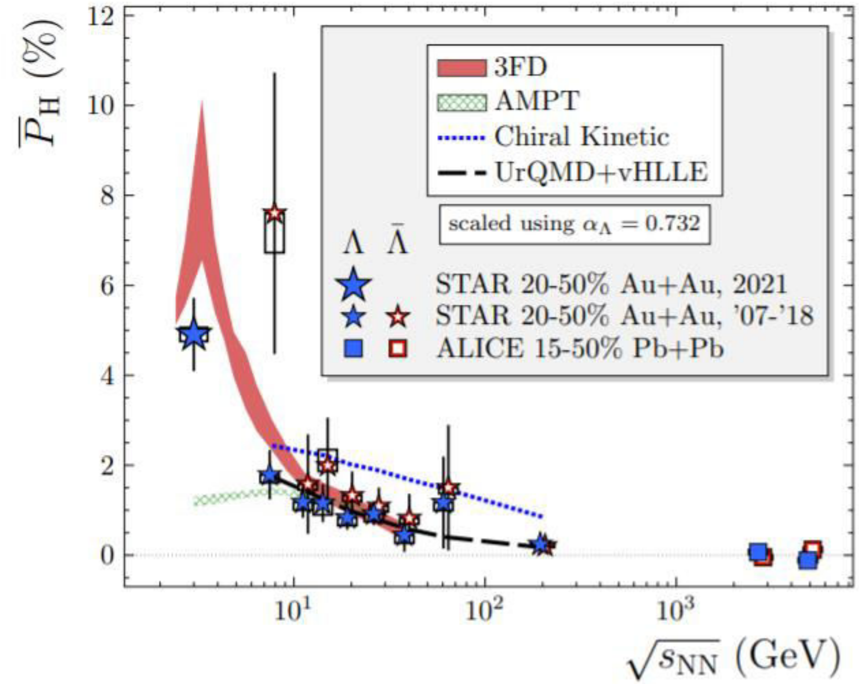

- Energy dependence of global polarization is reproduced by models: AMPT, 3FD, UrQMD+vHLLE
- AMPT with partonic transport strongly underestimates measurements at $\sqrt{s_{NN}}$ = 3 GeV → hadron gas?

More differential, centrality

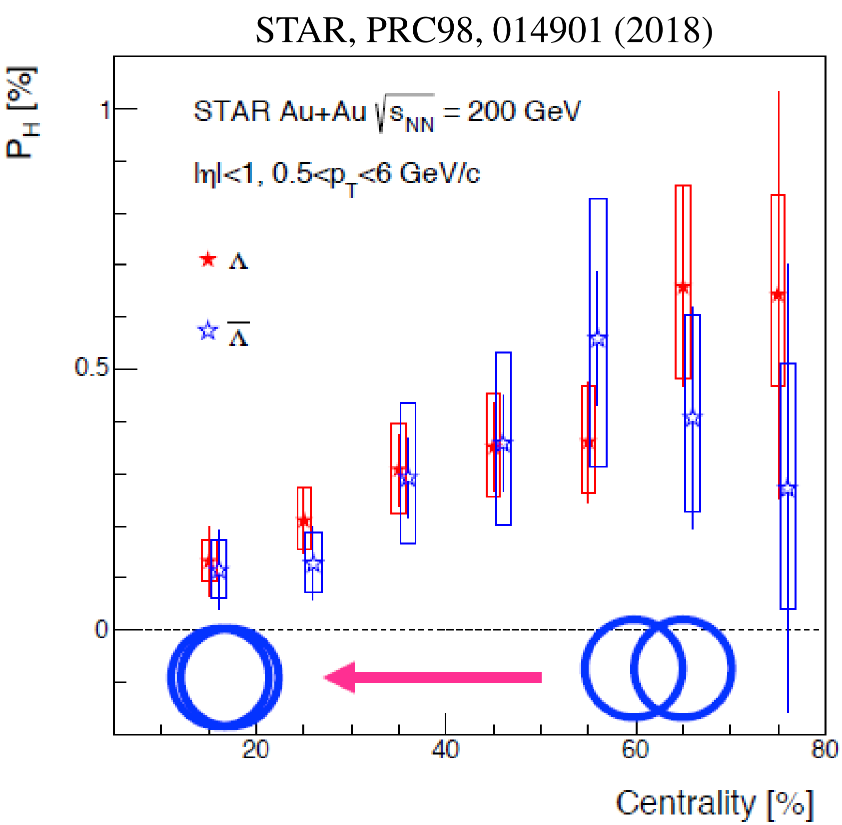

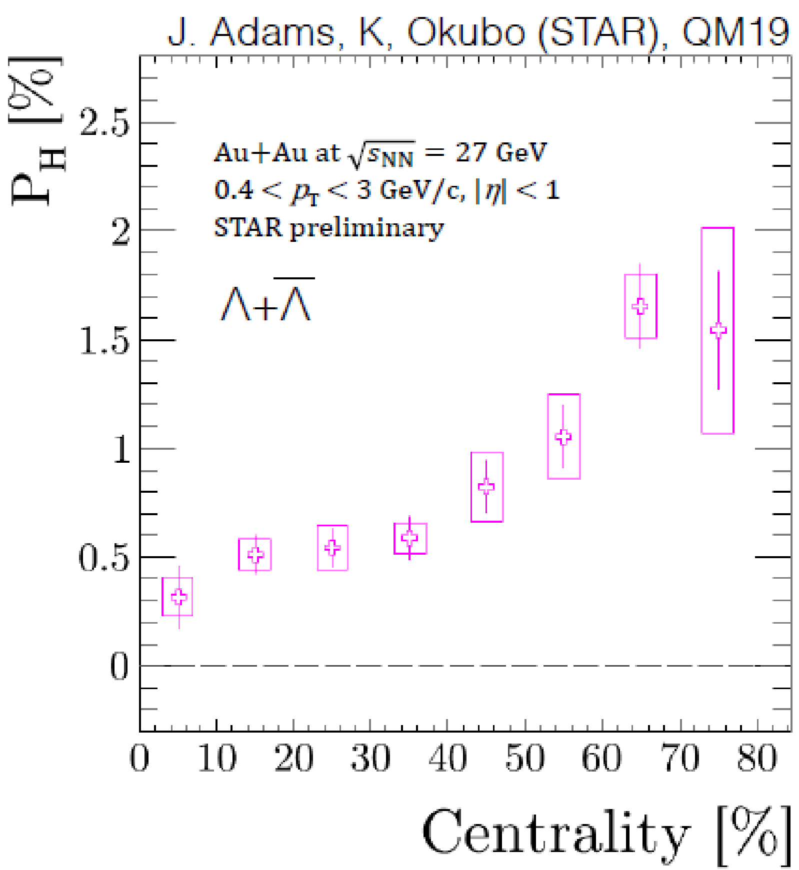

- Reduced polarization in most central collision → no initial angular momentum
- Similar trends at lower collision energies

More differential, rapidity

STAR, PRC98, 014901 (2018)

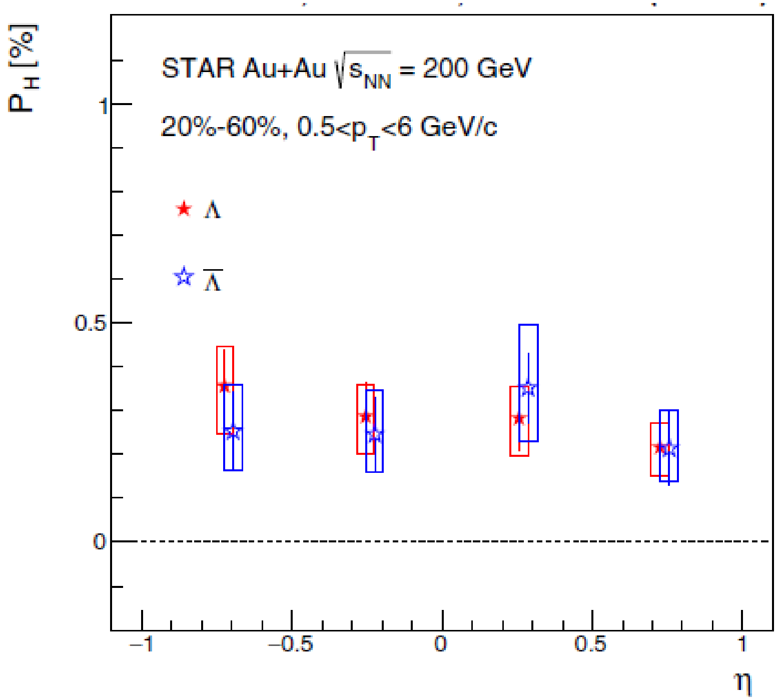

STAR, QM19

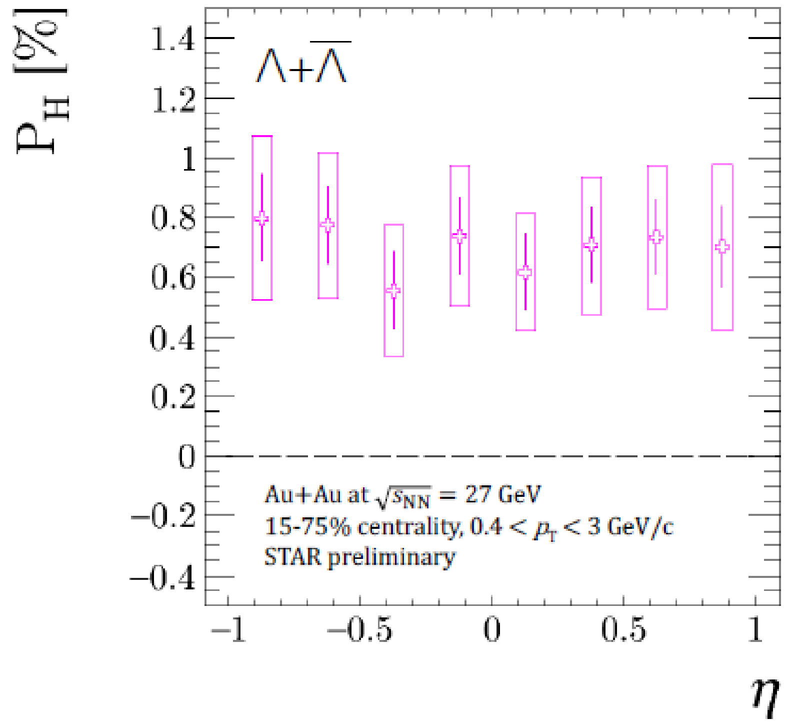

- No rapidity dependence observed at |η| < 1 within uncertainties
- Model predictions differ, wider η - coverage is needed

More differential, azimuthal angle

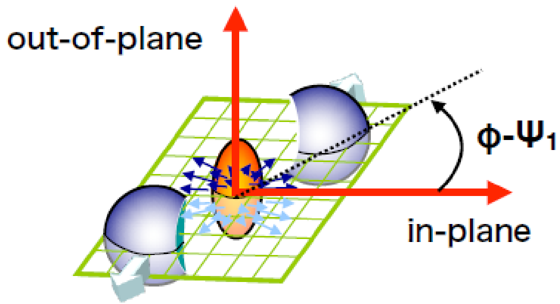

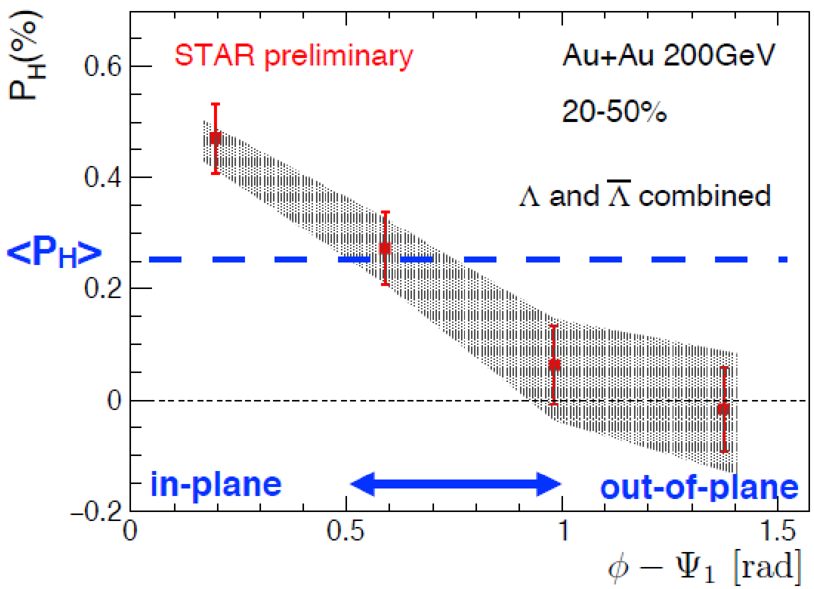

PRC 99 014905 (2019)
AMPT

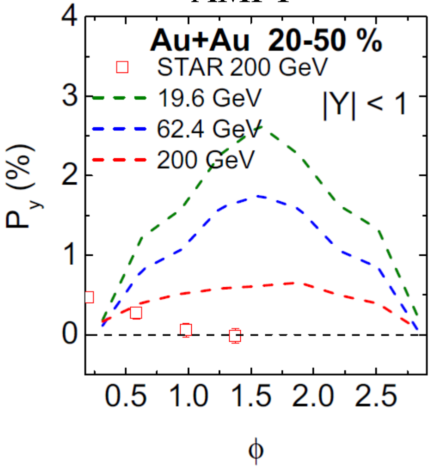

arXiv:2003.03640

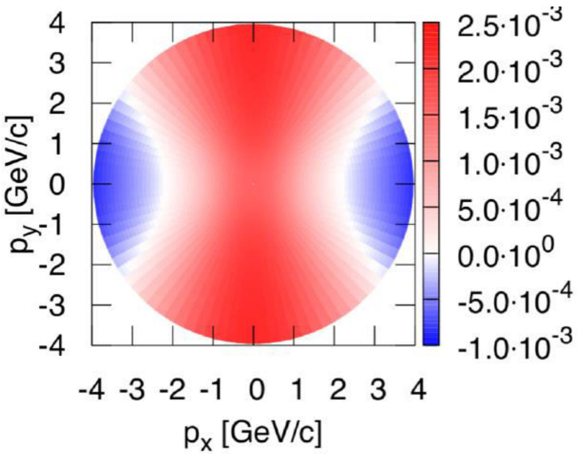

- Larger polarization is observed in-plane
- Models predict the opposite dependence and larger polarization out-of-plane
- Not fully understood

Polarization of Ξ and Ω

	Mass (GeV/c²)	cτ (cm)	decay mode	decay parameter	magnetic moment (μ_N)	spin
Λ (uds)	1.115683	7.89	Λ->πp (63.9%)	0.732±0.014	−0.613	1/2
Ξ^- (dss)	1.32171	4.91	Ξ^-->Λπ^- (99.887%)	−0.401±0.010	−0.6507	1/2
Ω^- (sss)	1.67245	2.46	Ω^-->ΛK^- (67.8%)	0.0157±0.002	-2.02	3/2

- Λ, Ξ and Ω have different spins and magnetic moments, different number of s-quarks, less feedback for heavier hyperons
- Direct measurements are difficult due to small values of α
- Measured based on polarization of daughter Λ

Phys. Rev. Lett. 126, 162301 (2021)

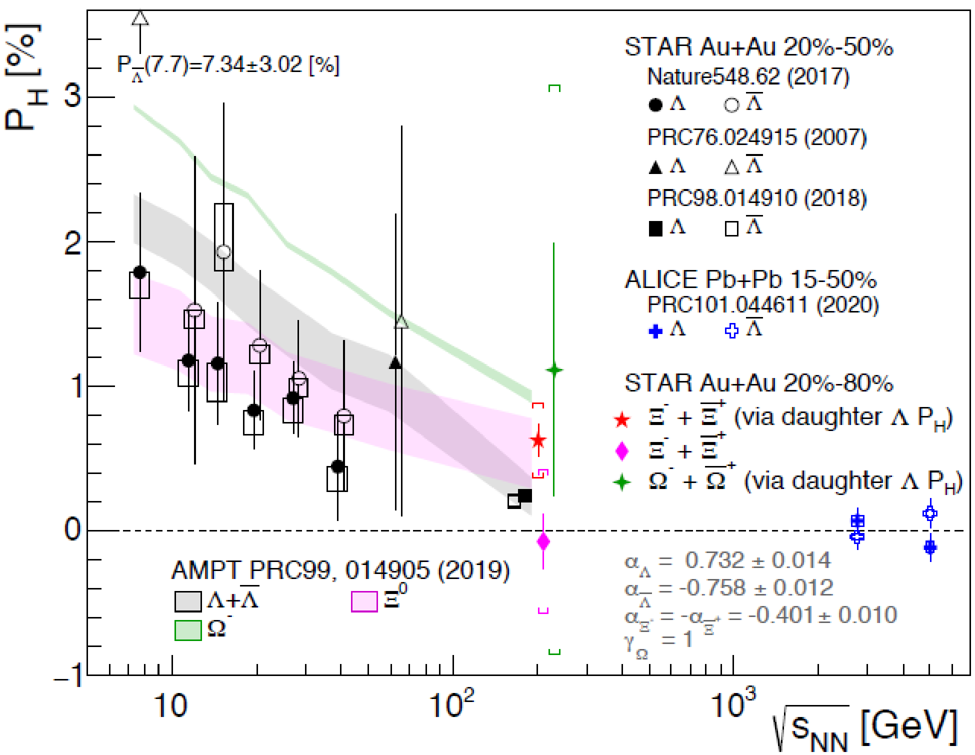

- AMPT is consistent with measurements
- Polarization of Ξ is larger compared with Λ:

$$\langle P_{\Lambda+\bar{\Lambda}}\rangle(\%) = 0.24 \pm 0.03 \pm 0.03$$

$$\langle P_{\Xi}\rangle = 0.47 \pm 0.10\ (\text{stat.}) \pm 0.23\ (\text{syst.})\ \%$$

- Λ results are not feed-back corrected (~ 15%)
- The AMPT is consistent with measurements
- Polarization of Ξ is larger compared with Λ
- Earlier freeze-out of multi-strange baryons is consistent with larger value of P_H for Ξ
- Large uncertainties for Ω, can expect larger signal, $P = \frac{\langle \bar{s} \rangle}{s} \sim \frac{s+1}{3} \frac{\bar{\omega}}{T}$ PRC95.054902 (2017)

Polarization along the beam direction, P_z

S. Voloshin, EPJ Web Conf.171, 07002 (2018)

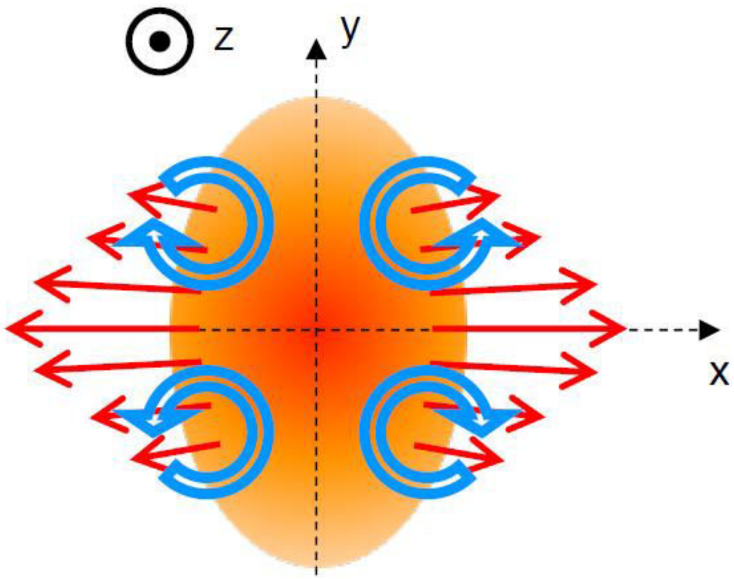

- v_2 which manifests itself in stronger flow in in-plane that in out-of-plane is a source of vorticity along the beam direction (z-axis)
- The vorticity and the corresponding polarization have azimuthal angle dependence (quadrupole structure) in the transverse plane - local polarization
- Use weak decays of hyperons to measure polarization

$$\Lambda \to p + \pi^-$$

θ_p^* = polar angle of daughter baryon in hyperon rest frame

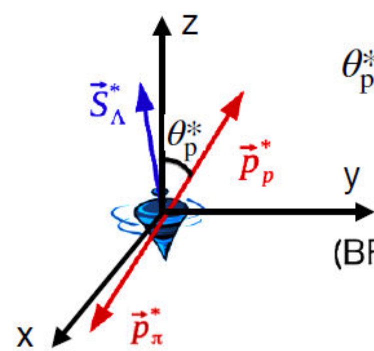

(BR: 63.9%, cτ~7.9 cm)

- This polarization can be characterized by the second harmonic sine component in the Fourier decomposition of the polarization along the beam axis (Pz) as a function of the particle azimuthal angle relative to the elliptic flow plane

$$P_{z,s2} = \langle P_z \sin(2\varphi - 2\Psi_2) \rangle$$

$$4\pi \frac{dN}{d\Omega^*} = 1 + \alpha_H \mathbf{P}_H \cdot \hat{\mathbf{p}}_p^* = 1 + \alpha_H P_H \cos\theta_p^*$$

$$P_z(p_T, y_H, \varphi) = \frac{\langle \cos\theta_p^* \rangle}{\alpha_H \langle (\cos\theta_p^*)^2 \rangle}$$

Phys. Rev. Lett. **123**, 132301

Polarization along the beam direction, P_z

arXiv:2107.11183 [nucl-ex]

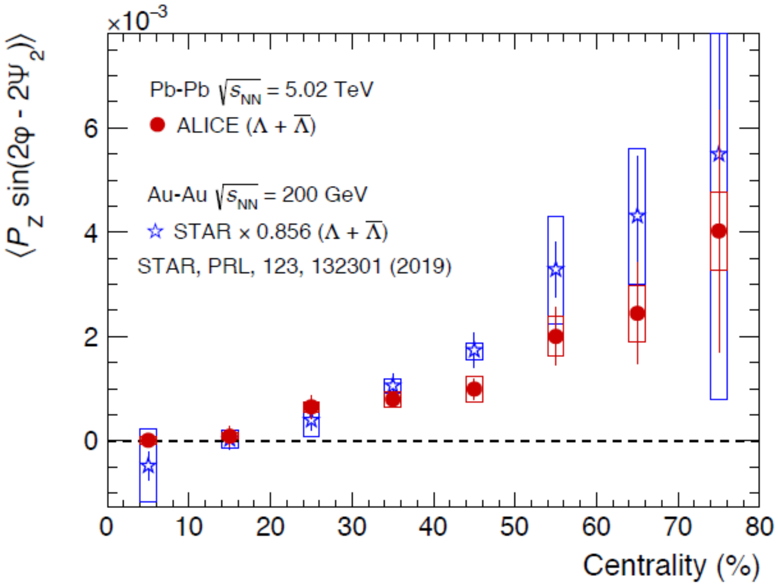

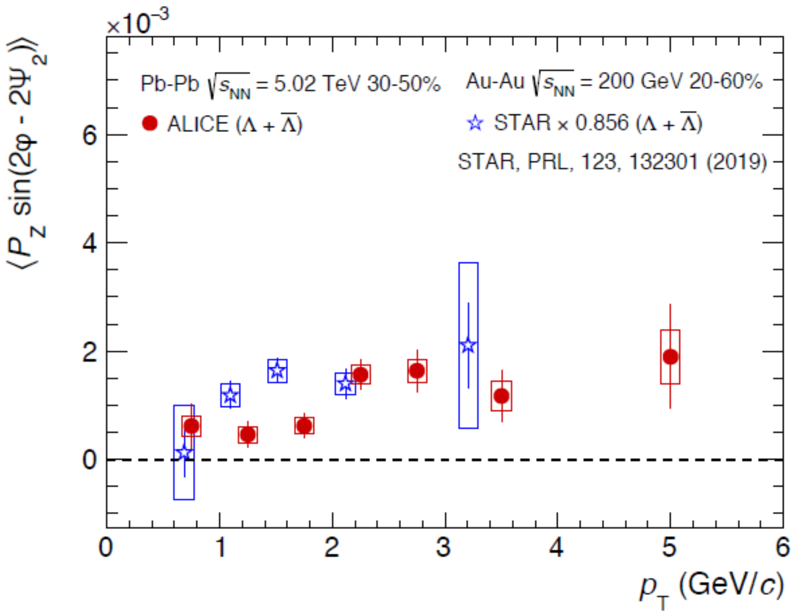

- P_z at the LHC is similar in magnitude compared to top RHIC energy (tends to be smaller in semicentral collisions)
- At p_T < 2.0 GeV/c, P_z at the LHC is smaller than the STAR results in semi-central collisions although $v_2(p_T)$ at top RHIC and the LHC energies are comparable
- The sign of phase modulation of P_z is the same at RHIC and the LHC

Polarization along the beam direction, P_z

Phys.Rev.Lett. 123 (2019) 13, 132301, S. Voloshin, EPJ Web Conf.171, 07002 (2018)

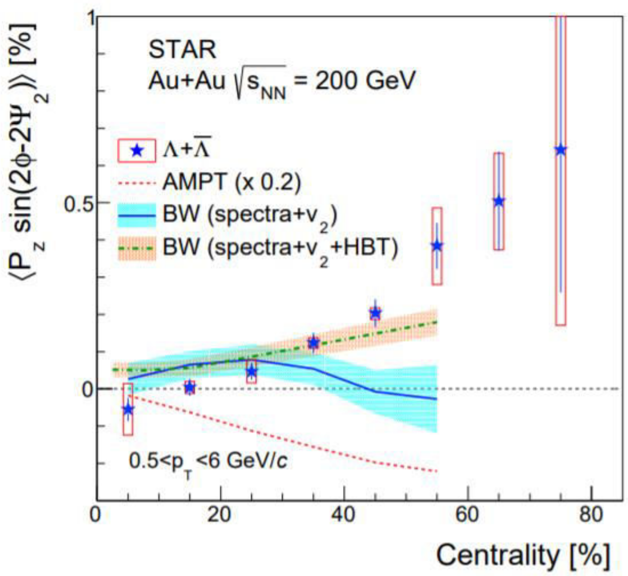

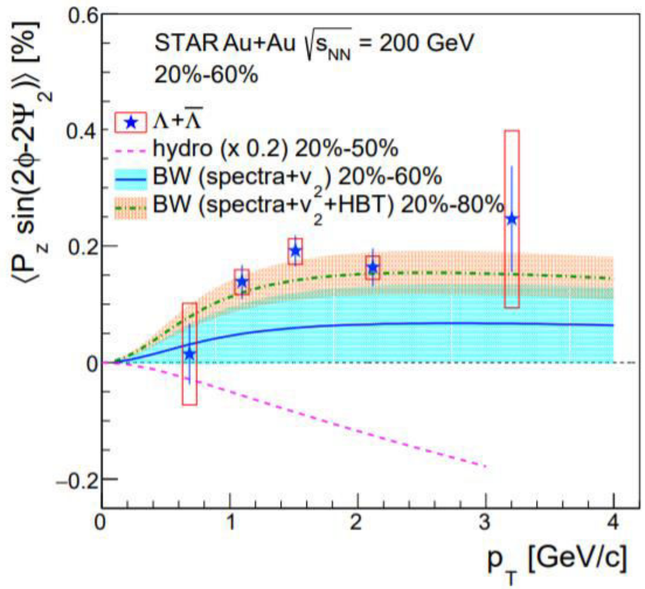

- Hydro-inspired BW model (kinematic vorticity, $\omega_z = \frac{1}{2}\left(\frac{\partial u_y}{\partial x} - \frac{\partial u_x}{\partial y}\right)$, *u* – local flow velocity) describes the data unlike more realistic models
- Hydro and transport models which describe the elliptic flow in heavy-ion collisions generate similar amplitude but different sign P_z (“spin sign puzzle”).

Spin alignment for vector mesons

Species	K^{*0}	φ
Quark content	$\bar{d}s$	$s\bar{s}$
Mass (MeV/c²)	896	1020
Lifetime (fm/c)	4	45
Spin (J^P)	1^-	1^-
Decays	Kπ	KK
Branching ratio	~100%	66%

Zuo – Tang Liang, Xin – Nian Wang, Phys. Lett. B629: 20 – 26,2005

$$\boxed{\frac{dN}{dcos\theta} = N_0[1 - \rho_{0,0} + cos^2\theta(3\rho_{0,0} - 1)]}$$

$\rho_{0,0}$ is a probability for vector meson to be in spin state = 0

$$\rho_{00} = 1/[3 + (\omega/T)^2]$$

- Quantization axis:
  - ✓ normal to the event plane (impact parameter and beam axis)
  - ✓ normal to the production plane (momentum of the vector meson and the beam axis)

$$\boxed{\rho_{00}\,(\mathrm{PP}) - \frac{1}{3} = [\rho_{00}\,(\mathrm{EP}) - \frac{1}{3}]\,[\frac{1+3v_2}{4}]}$$

- Expectations:
  - ✓ To be observed at low p_T where hadronization via recombination dominates
  - ✓ small signal for central and peripheral collisions, maximum effect for mid-central collisions

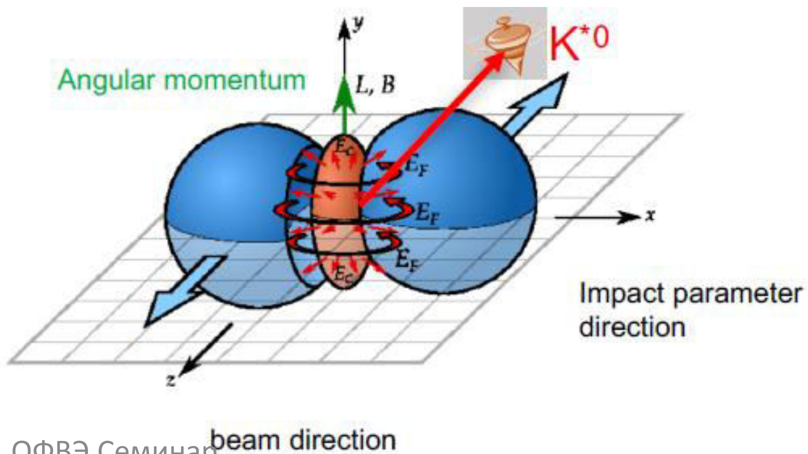

Reconstruction of vector mesons

- Invariant mass method, mixed-event spectrum for uncorrelated combinatorial background
- Resonance peaks are described with Voigitian function, remaining background with polynomials after subtraction of uncorrelated combinatorial background

PRC 95, 064606 (2017); PRC 91 024609 (2015)

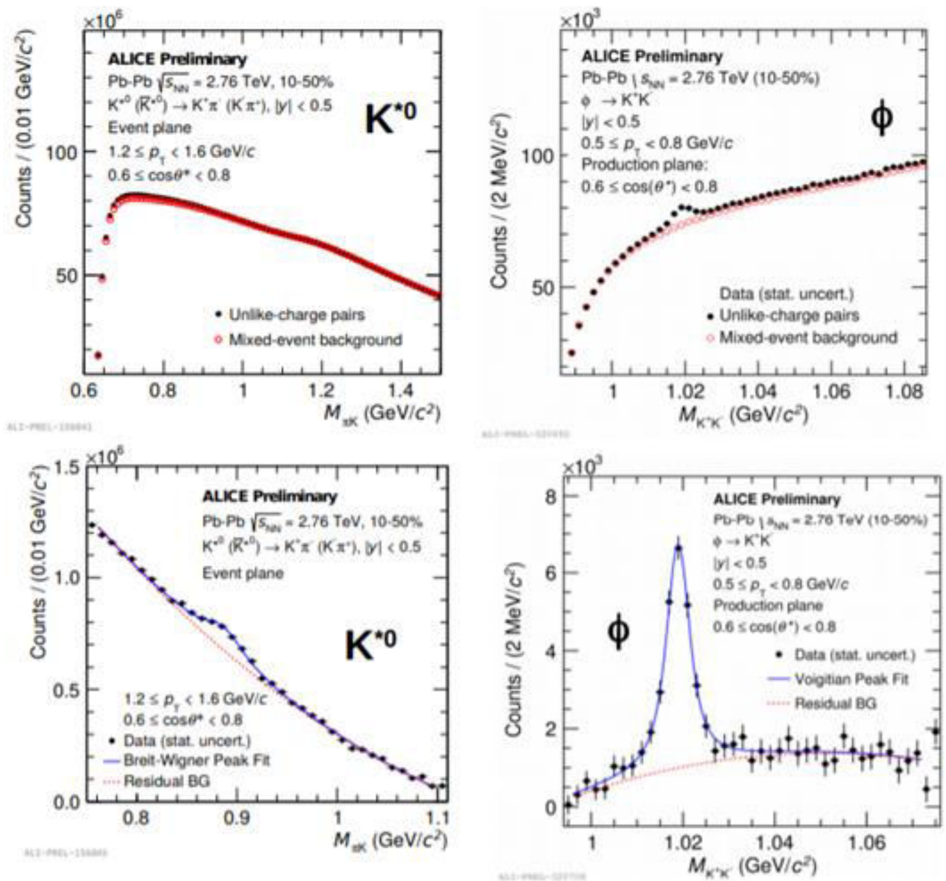

Angular distributions

PRL 125, 012301 (2020)

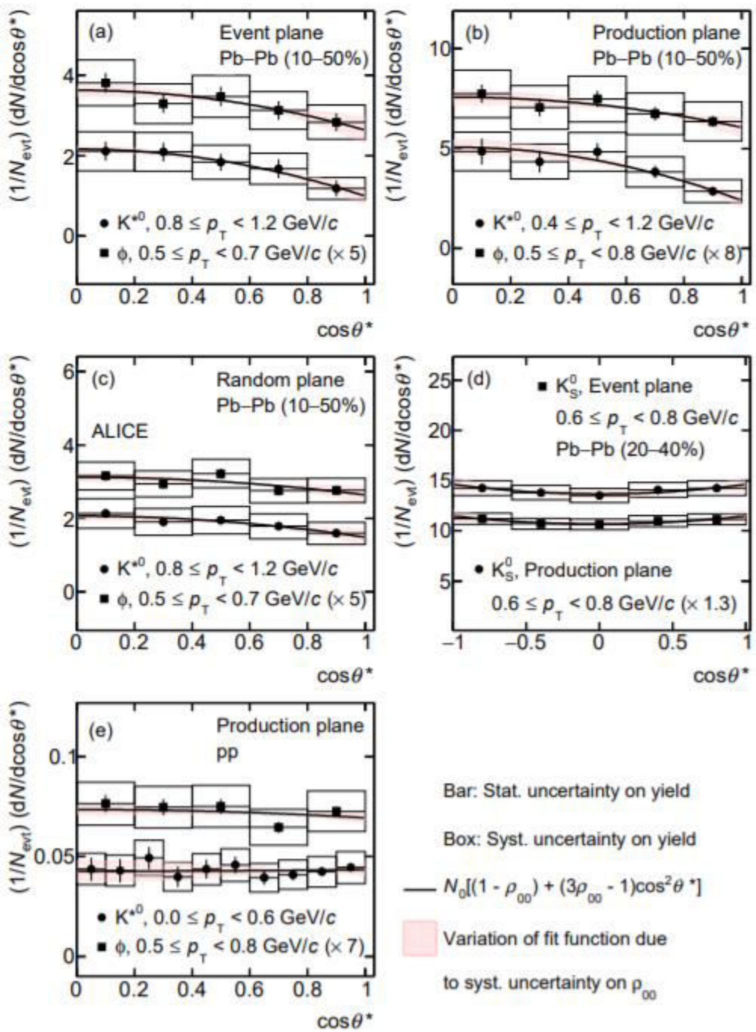

- Not flat distributions with respect to EP and PP quantization axis for vector mesons in non-central heavy-ion collisions

- Flat angular distributions:
  - ✓ for vector mesons with respect to random quantization axis in heavy ion collisions
  - ✓ for neutral K_S^0 with respect to any axis in heavy-ion collisions
  - ✓ For vector mesons and K_S^0 in pp collisions

Results for K^{*0} and ϕ vs. p_T

PRL 125, 012301 (2020)

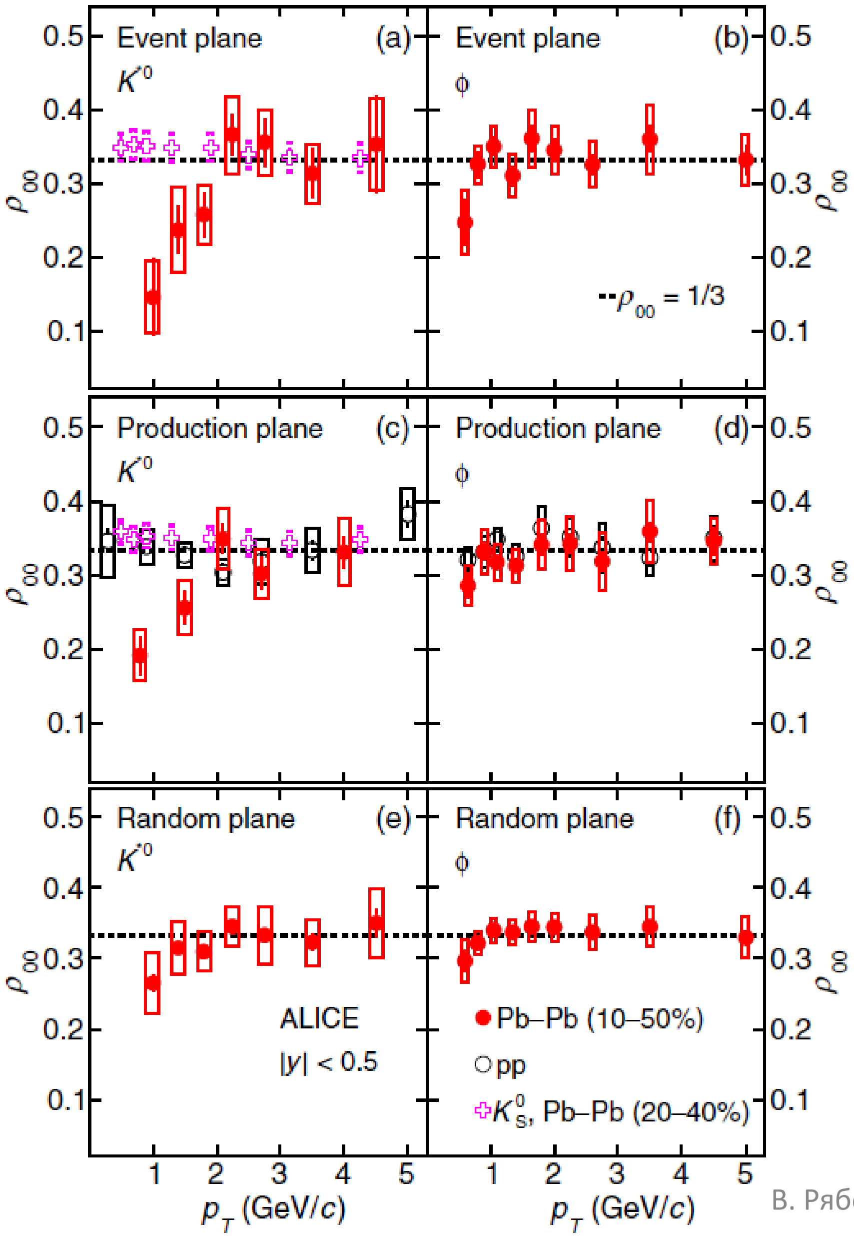

- ρ_{00} ~ 1/3 for:
  - ✓ $p_T(K^{*0})$ > 2 GeV/c and $p_T(\phi)$ > 0.8 GeV/c
  - ✓ K_S^0 with zero spin
  - ✓ K^{*0} and ϕ in pp collisions
  - ✓ K^{*0} and ϕ with random plane in Pb-Pb@2.76
- ρ_{00} < 1/3 for K^{*0} and ϕ at low p_T in semi-central Pb-Pb@2.76 collisions

Results for K^{*0} and ϕ vs. p_T

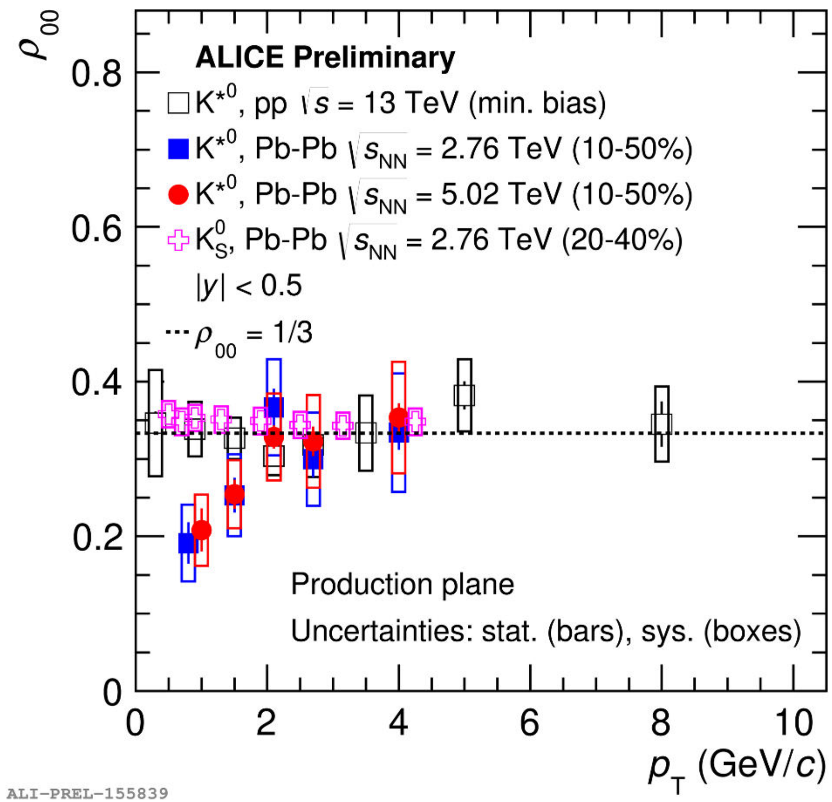

- Results are now confirmed with new preliminary measurements for K^{*0} in Pb-Pb@5.02 TeV

Results for K^{*0} and ϕ vs. centrality

PRL 125, 012301 (2020)

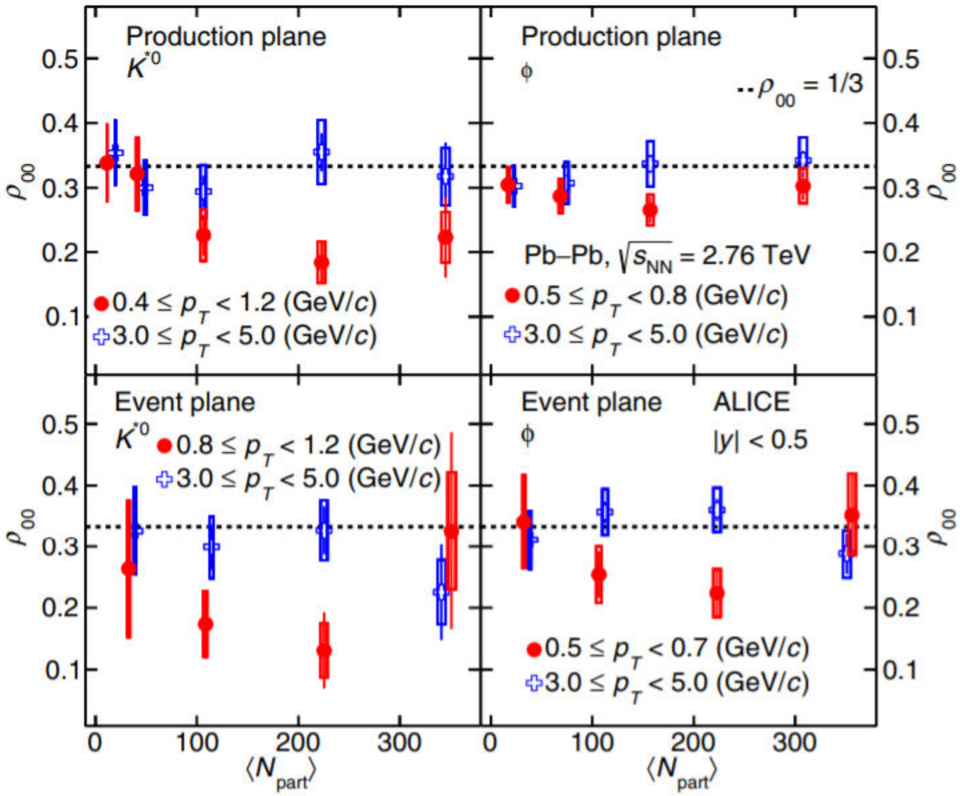

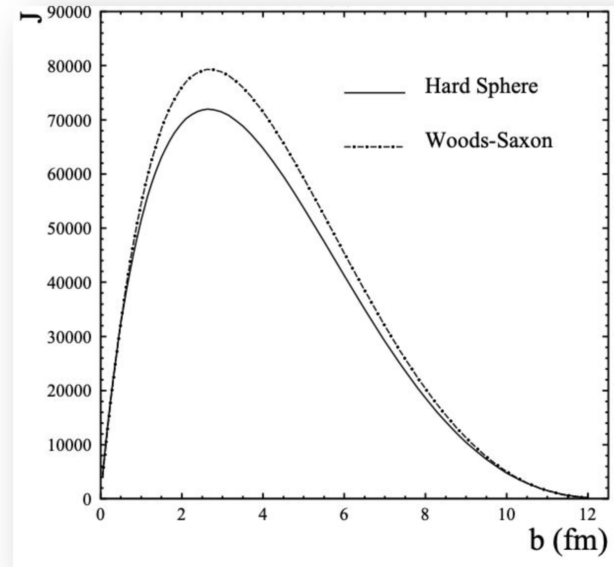

- Low p_T (0.8-1.2 GeV/c for K^{*0} and 0.5-0.7 GeV/c for ϕ):
  - ✓ ρ_{00} < 1/3 in semi-central PbPb@2.76 by 2-3 σ
  - ✓ follows centrality dependence of angular momentum
- High p_T (3-5 GeV/c):
  - ✓ $\rho_{00} \sim 1/3$

Results for p_T and centrality dependence of ρ_{00} are qualitatively consistent with quark recombination in a polarized medium

Energy dependence

NPA 1005 (2021) 121733, Singha et al.

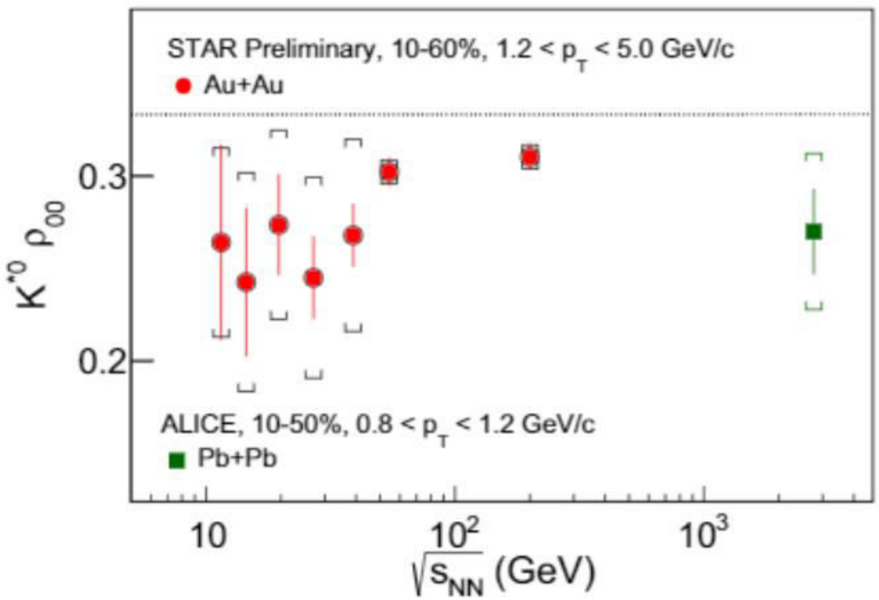

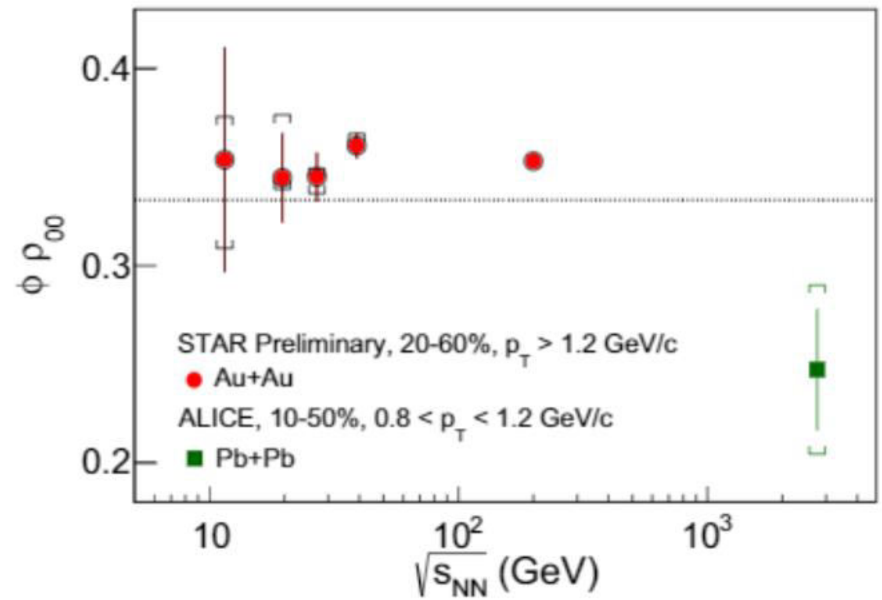

- ρ_{00} for K^{*0} is smaller than 1/3 at low p_T in semi-central heavy-ion collisions; no significant collision energy dependence within uncertainties
- ρ_{00} for ϕ is > 1/3 at RHIC and is < 1/3 at the LHC
- Observed large deviation of ρ_{00} from 1/3 challenges theoretical understanding → ρ_{00} can depend on multiple physics mechanisms (vorticity, magnetic field, hadronization scenarios, lifetimes and masses of the particles etc.) → more theoretical efforts are required for understanding of the data

Conclusions

- Polarization effects were predicted and experimentally observed in non-central heavy-ion collisions in a wide energy range:
  - ✓ global polarization of $\Lambda(\overline{\Lambda})$ hyperons, energy dependence is reproduced by theoretical models, a sign problem for azimuthal dependence
  - ✓ first measurements of global polarization for Ξ (s=1/2, slightly higher that Λ) and Ω (s = 3/2, large uncertainties)
  - ✓ local polarization related to v_2 is observed, "spin sign puzzle"
  - ✓ evidence of spin alignment for vector mesons related to initial angular momentum spin alignment, not observed for spin = 0 particles and in pp
- Many open questions remain, more precise measurements are needed for better understanding of the nature of polarization in heavy-ion collisions

BACKUP

Feed-down effect

- ~60% of measured Λ are feed-down from $\Sigma^* \to \Lambda\pi$, $\Sigma^0 \to \Lambda\gamma$, $\Xi \to \Lambda\pi$
- Polarization of parent particle R is transferred to its daughter Λ (Polarization transfer could be negative!)

$$\mathbf{S}^*_\Lambda = C\mathbf{S}^*_R \qquad \langle S_y \rangle \propto \frac{S(S+1)}{3}(\omega + \frac{\mu}{S}B)$$

$C_{\Lambda R}$: coefficient of spin transfer from parent R to Λ
S_R : parent particle's spin
$f_{\Lambda R}$: fraction of Λ originating from parent R
μ_R : magnetic moment of particle R

$$\begin{pmatrix} \varpi_c \\ B_c/T \end{pmatrix} = \begin{bmatrix} \frac{2}{3}\sum_R \left(f_{\Lambda R}C_{\Lambda R} - \frac{1}{3}f_{\Sigma^0 R}C_{\Sigma^0 R}\right) S_R(S_R+1) & \frac{2}{3}\sum_R \left(f_{\Lambda R}C_{\Lambda R} - \frac{1}{3}f_{\Sigma^0 R}C_{\Sigma^0 R}\right)(S_R+1)\mu_R \\ \frac{2}{3}\sum_{\overline{R}} \left(f_{\overline{\Lambda R}}C_{\overline{\Lambda R}} - \frac{1}{3}f_{\overline{\Sigma^0}\overline{R}}C_{\overline{\Sigma^0}\overline{R}}\right) S_{\overline{R}}(S_{\overline{R}}+1) & \frac{2}{3}\sum_{\overline{R}} \left(f_{\overline{\Lambda R}}C_{\overline{\Lambda R}} - \frac{1}{3}f_{\overline{\Sigma^0}\overline{R}}C_{\overline{\Sigma^0}\overline{R}}\right)(S_{\overline{R}}+1)\mu_{\overline{R}} \end{bmatrix}^{-1} \begin{pmatrix} P^{\mathrm{meas}}_\Lambda \\ P^{\mathrm{meas}}_{\overline{\Lambda}} \end{pmatrix}$$

Becattini, Karpenko, Lisa, Upsal, and Voloshin, PRC95.054902 (2017)

Decay	C
Parity conserving: $1/2^+ \to 1/2^+\ 0^-$	$-1/3$
Parity conserving: $1/2^- \to 1/2^+\ 0^-$	1
Parity conserving: $3/2^+ \to 1/2^+\ 0^-$	1/3
Parity-conserving: $3/2^- \to 1/2^+\ 0^-$	$-1/5$
$\Xi^0 \to \Lambda + \pi^0$	+0.900
$\Xi^- \to \Lambda + \pi^-$	+0.927
$\Sigma^0 \to \Lambda + \gamma$	$-1/3$

Primary Λ polarization will be diluted by 15%-20% (model-dependent)
This also suggests that **the polarization of daughter particles can be used to measure their parent polarization!** e.g. Ξ, Ω

T. Niida, NA61/SHINE Open Seminar 2021 15

Ξ and Ω polarization measurements

$$\frac{dN}{d\Omega^*} = \frac{1}{4\pi}\left(1 + \alpha_H \mathbf{P}_H^* \cdot \hat{\boldsymbol{p}}_B^*\right)$$

Getting difficult due to smaller decay parameter for Ξ and Ω…

$$\alpha_\Lambda = 0.732,\ \ \alpha_{\Xi^-} = -0.401,\ \ \alpha_{\Omega^-} = 0.0157$$

spin 1/2

Polarization of daughter Λ in a weak decay of Ξ:
(based on Lee-Yang formula)

T.D. Lee and C.N. Yang, Phys. Rev.108.1645 (1957)

$$\mathbf{P}_\Lambda^* = \frac{(\alpha_\Xi + \mathbf{P}_\Xi^* \cdot \hat{p}_\Lambda^*)\hat{p}_\Lambda^* + \beta_\Xi \mathbf{P}_\Xi^* \times \hat{p}_\Lambda^* + \gamma_\Xi \hat{p}_\Lambda^* \times (\mathbf{P}_\Xi^* \times \hat{p}_\Lambda^*)}{1 + \alpha_\Xi \mathbf{P}_\Xi^* \cdot \hat{p}_\Lambda^*}$$

$$\alpha^2 + \beta^2 + \gamma^2 = 1$$

$$\mathbf{P}_\Lambda^* = C_{\Xi^-\Lambda}\mathbf{P}_\Xi^* = \tfrac{1}{3}\left(1 + 2\gamma_\Xi\right)\mathbf{P}_\Xi^*.$$

$$C_{\Xi^-\Lambda} = +0.944$$

spin 3/2

Similarly, daughter Λ polarization from Ω:

$$\mathbf{P}_\Lambda^* = C_{\Omega^-\Lambda}\mathbf{P}_\Omega^* = \tfrac{1}{5}\left(1 + 4\gamma_\Omega\right)\mathbf{P}_\Omega^*.$$

Here **γ_Ω is unknown**.
- Time-reversal violation parameter β_Ω would be small
- α_Ω is very small

then $\gamma_\Omega \sim \pm 1$ and the polarization transfer $C_{\Omega\Lambda}$ leads to:

$$C_{\Omega\Lambda} \approx +1 \text{ or } -0.6$$

Parent particle polarization can be studied by measuring daughter particle polarization!

T. Niida, NA61/SHINE Open Seminar 2021 26

Highlights in the CERN Courier

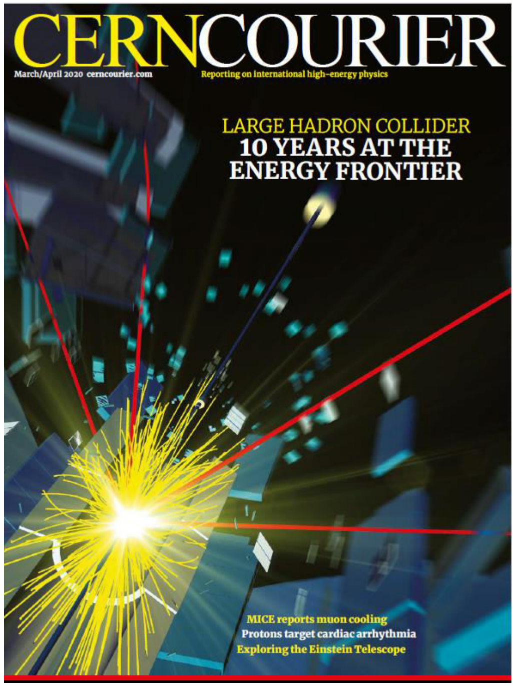

ALICE

Plasma polarised by spin–orbit effect

Spin–orbit coupling causes fine structure in atomic physics and shell structure in nuclear physics, and is a key ingredient in the field of spintronics in materials sciences. It is also expected to affect the development of the quickly rotating quark–gluon plasma (QGP) created in non-central collisions of lead nuclei at LHC energies. As such, plasmas are created by the collisions of lead nuclei that almost miss each other. They have very high angular momenta of the order of $10^7\hbar$ – equivalent to the order of 10^{21} revolutions per second. While the extreme magnetic fields generated by spectating nucleons (of the order of 10^{14} T, *CERN Courier* Jan/Feb 2020 p17) quickly decay as the spectator nucleons pass by, the plasma's angular momentum is sustained throughout the evolution of the system as it is a conserved quantity. These extreme angular momenta are expected to lead to spin–orbit interactions that polarise the quarks in the plasma along the direction of the angular momentum of the plasma's rotation. This should in turn cause the spins of vector (spin-1) mesons to align if hadronisation proceeds via the recombination of partons or by fragmentation. To study this effect, the ALICE collaboration recently measured the spin alignment of the decay products of neutral K^* and ϕ vector mesons produced in non-central Pb–Pb collisions.

Spin alignment can be studied by measuring the angular distribution of the decay products of the vector mesons. It is quantified by the probability ρ_{00} of finding a vector meson in a spin state 0 with respect to the direction of the angular momentum of the rotating QGP, which is approximately perpendicular to the plane of the beam direction and the impact parameter of the two colliding nuclei. In the absence of spin-alignment effects, the probability of finding a vector meson in any of the three spin states (–1, 0, 1) should be equal, with $\rho_{00} = 1/3$.

The ALICE collaboration measured the angular distributions of neutral K^* and ϕ vector mesons via their hadronic decays to $K\pi$ and KK pairs, respectively. ρ_{00} was found to deviate from 1/3 for low-p_T and mid-central collisions at a level of 3σ (figure 1). The corresponding results for ϕ mesons show a deviation of ρ_{00} values from 1/3 at a level of 2σ. The observed p_T dependence of ρ_{00} is expected if quark polarisation via spin–orbit coupling is subsequently transferred to the vector mesons by hadronisation, via the recombination of a quark and an anti-quark from the quark–gluon plasma. The data are also consistent with the initial angular momentum of the hot and dense matter being highest for mid-central collisions and decreasing towards zero for central and peripheral collisions.

The results are surprising, however, as corresponding quark-polarisation values obtained from studies with Λ hyperons are compatible with zero. A number of systematic tests have been carried out to verify these surprising results. K^0_S mesons do indeed yield $\rho_{00} = 1/3$, indicating no spin alignment, as must be true for a spin-zero particle. For proton–proton collisions, the absence of initial angular momentum also leads to $\rho_{00} = 1/3$, consistent with the observed neutral K^* spin alignment being the result of spin–orbit coupling.

The present measurements are a step towards experimentally establishing possible spin–orbit interactions in the relativistic-QCD matter of the quark–gluon plasma. In the future, higher statistics measurements in Run 3 will significantly improve the precision, and studies with the charged K^*, which has a magnetic moment seven times larger than neutral K^*, may even allow a direct observation of the effect of the strong magnetic fields initially experienced by the quark–gluon plasma.

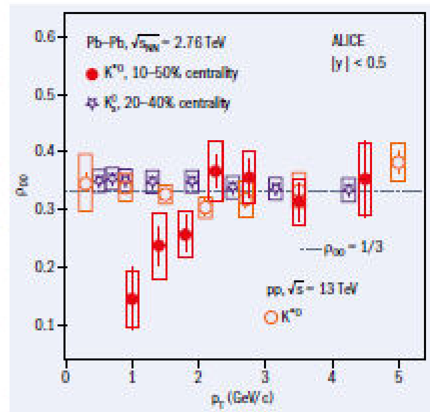

Fig. 1. *The spin alignment of (spin-1) K^{*0} mesons (red circles) can be characterised by deviations from $\rho_{00} = 1/3$, which is estimated here versus their transverse momenta, p_T. The same variable was estimated for (spin-0) K^0_S mesons (magenta stars), and K^{*0} mesons produced in proton–proton collisions with negligible angular momentum (hollow orange circles), as systematic tests.*

Further reading

ALICE Collab. 2019 arXiv:1910.14408.
ALICE Collab. 2019 arXiv:1909.01281.

Relation between EP and PP

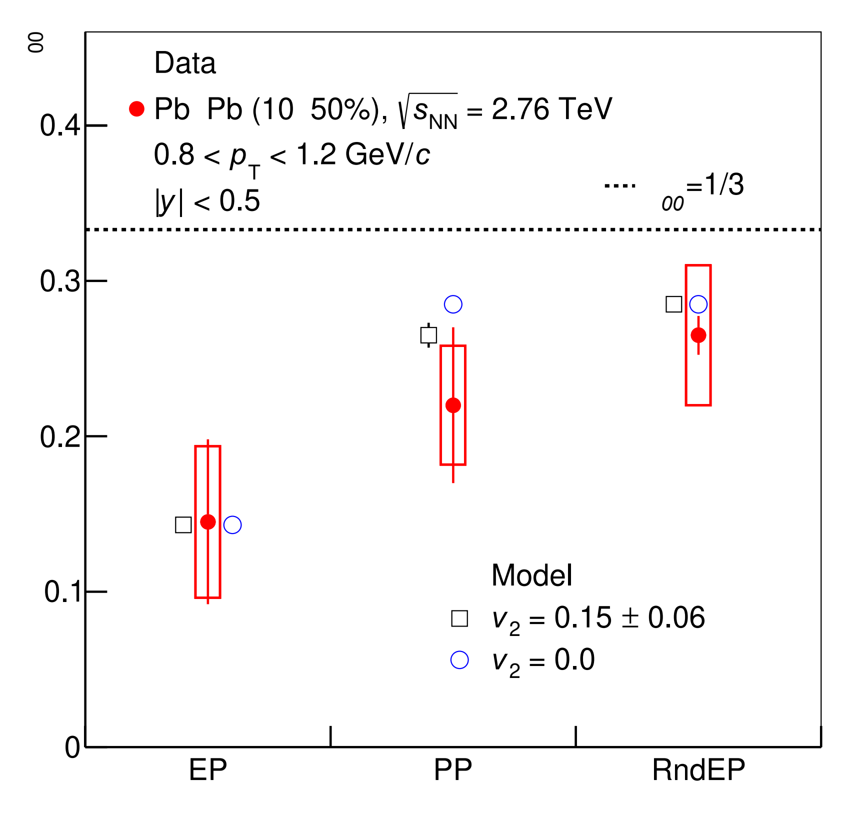

$$\rho_{00}\,(PP) - \frac{1}{3} = [\rho_{00}\ (EP) - \frac{1}{3}]\ [\frac{1+3v_2}{4}]$$

The physical picture is that spin alignment with respect to the event plane is coupled to that in the production plane through the elliptic flow of the system.

The ρ_{00}(RndEP) is lower than 1/3 as the quantization axis is always perpendicular to the beam axis, resulting in a residual effect.

arXiv:1910.14408 (ALICE)

Directed flow v_1

STAR, Phys. Rev. C 98, 014915

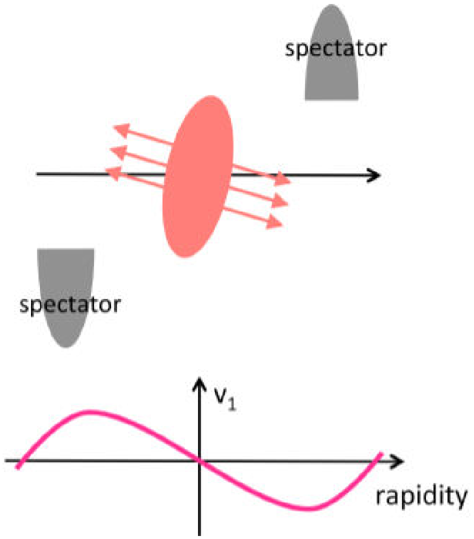

$$\frac{d^3N}{dp_t\,dy\,d\Delta\varphi} = \frac{d^2N}{dp_t\,dy}\frac{1}{2\pi}\left(1 + 2v_1\cos(\Delta\varphi) + 2v_2\cos(2\Delta\varphi) + \ldots\right)$$

Directed flow

Elliptic flow

$$\Delta\varphi = \varphi - \Psi_{RP}$$

- No single model that satisfactorily explains the directed flow dependencies on centrality, collision energy, system size, rapidity, transverse momentum and particle type
- The directed flow originates in the initial-state spatial and momentum (initial collective velocity fields) asymmetries in the transverse plane → tilted source initial conditions
- To describe the v_1 in heavy-ion collisions requires accounting for vorticity

PRL 108, 202301 (2012)

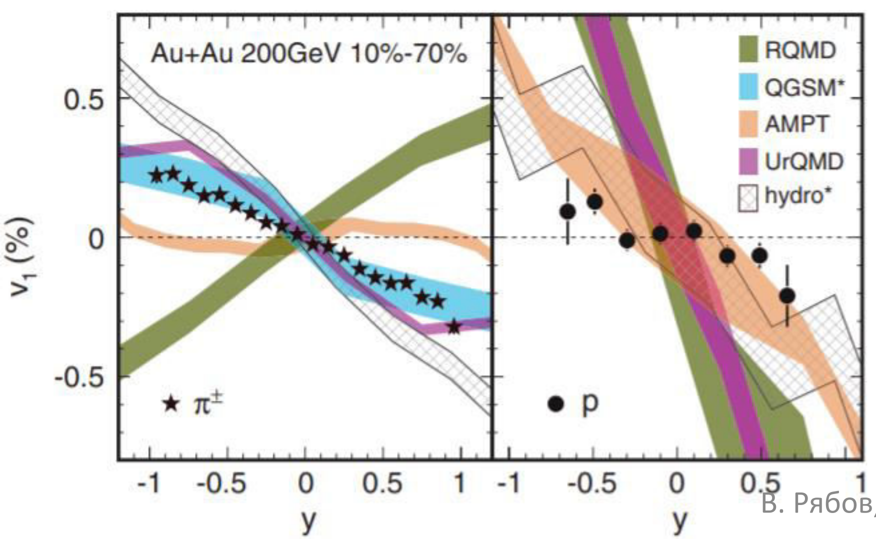

Becattini et al, Eur. Phys. J. C 78, 354 (2018)

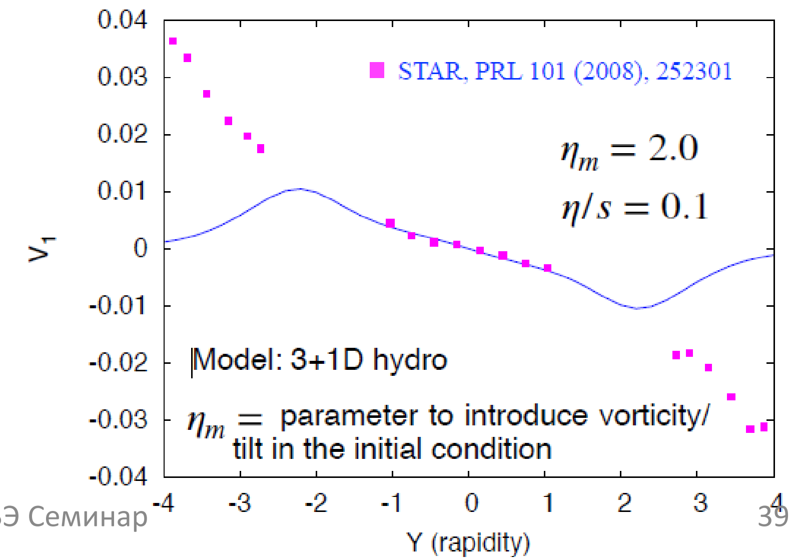

Different polarization for Λ and $\bar{\Lambda}$

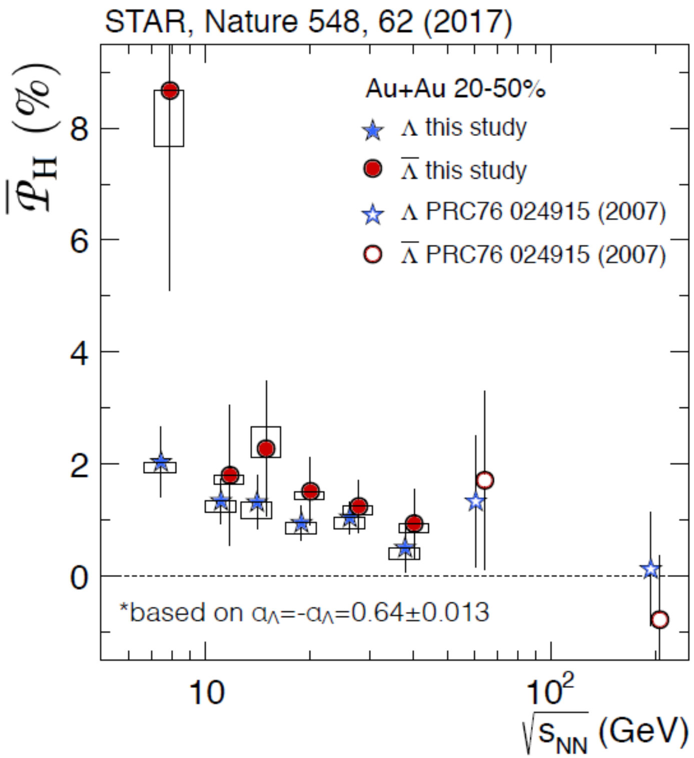

- Non-zero baryon potential can hardly explain the polarization difference for Λ and $\bar{\Lambda}$

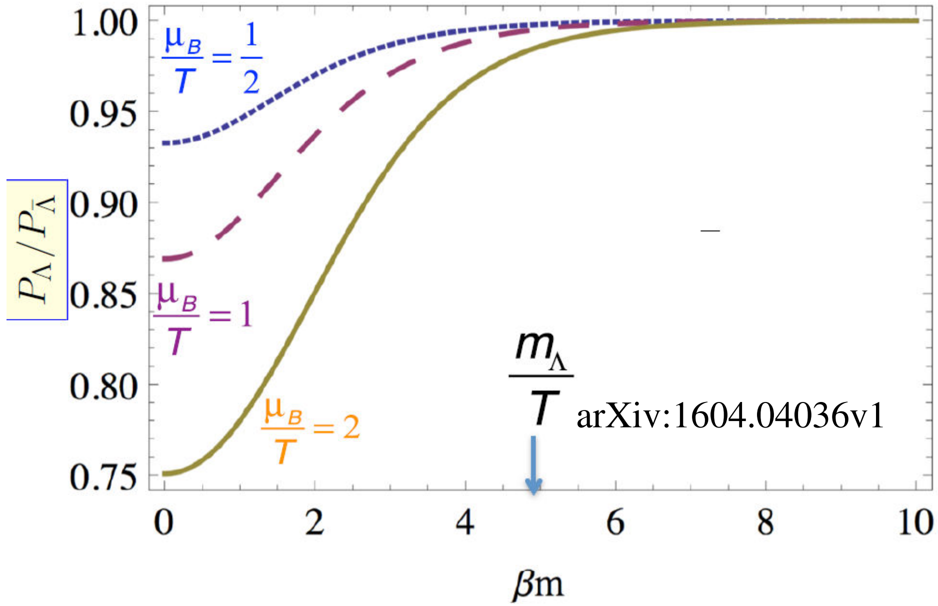

- B estimates are within the range of theoretical predictions

$$P_\Lambda \simeq \frac{1}{2}\frac{\omega}{T} + \frac{\mu_\Lambda B}{T}$$

$$P_{\bar{\Lambda}} \simeq \frac{1}{2}\frac{\omega}{T} - \frac{\mu_\Lambda B}{T}$$

μ_Λ - magnetic moment

$B = (P_\Lambda - P_{\bar{\Lambda}})\cdot T/(2\,\mu_\Lambda) \sim 2\cdot 10^{11}$ T or $eB \sim 10^2\, m_\pi^2$

$(P_\Lambda - P_{\bar{\Lambda}}) = 0.5\%$, T = 160 MeV at hadronization

- $\Lambda - \bar{\Lambda}$

Disagreement in P_z sign

Opposite sign

- UrQMD IC + hydrodynamic model
  F. Becattini and I. Karpenko, PRL.120.012302 (2018)
- AMPT
  X. Xia, H. Li, Z. Tang, Q. Wang, PRC98.024905 (2018)

Same sign

- Chiral kinetic approach
  Y. Sun and C.-M. Ko, PRC99, 011903(R) (2019)
- High resolution (3+1)D PICR hydrodynamic model
  Y. Xie, D. Wang, and L. P. Csernai, EPJC80.39 (2020)
- Blast-wave model
  S. Voloshin, EPJ Web Conf.171, 07002 (2018), STAR, PRL123.13201

Partly (one of component showing the same sign)

- Glauber/AMPT IC + (3+1)D viscous hydrodynamics
  H.-Z. Wu et al., Phys. Rev. Research 1, 033058 (2019)
- Thermal model
  W. Florkowski et al., Phys. Rev. C 100, 054907 (2019)

T. Niida, NA61/SHINE Open Seminar 2021

Vorticity vs. J

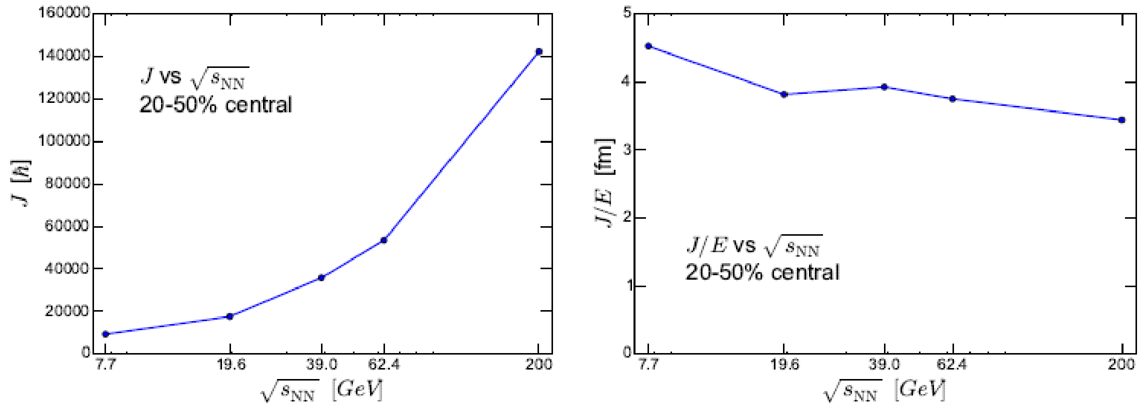

Fig. 11 Total angular momentum of the fireball (left) and total angular momentum scaled by total energy of the fireball (right) as a function of collision energy, in UrQMD+vHLLE calculation for 20-50% central Au-Au collisions.